Schwann Cells and Myelin in the Peripheral Nervous System

5

5.1 Normal Structure and Function of Schwann Cells and Myelin

Schwann cells (SCs) are derived from the neural crest (Webster 1993) and encircle all peripheral nerve axons. Functionally, two populations of Schwann cells can be identified, those producing myelin and those associated with unmyelinated axons. Because this distinction is fundamental to the appearance and physiology of SCs, the two types will be discussed separately. Schwann cells associated with unmyelinated fibers have been called Remak cells, but we will refer to them as nonmyelinating Schwann cells (NMSCs) because whether an SC produces myelin or not depends not on some critical and irreversible decision made in the process of differentiation, but on signals (likely neuregulin; Birchmeier and Nave (2008)) originating from its axon and related to its caliber (Weinberg and Spencer 1976; Aguayo et al. 1976; Pereira et al. 2012; Quintes et al. 2010). Axonal neuregulin signals information about axon size to Schwann cells; hypomyelination and hypermyelination result from reduced and overexpression of neuregulin, respectively (Michailov et al. 2004). Rarely, an unmyelinated axon develops one or more short myelinated internodes along its course, a phenomenon described particularly in aged animals (Heath 1982). Schwann cell biology has been the subject of a series of reviews collected in a special issue of Glia (Woodhoo and Sommer 2008).

5.1.1 Myelinating Schwann Cells

A myelinated fiber consists of an axon and its longitudinally arrayed series of SCs contained within a continuous basement membrane tube (the "Schwann tube"). Defined as that segment of the nerve fiber myelinated by a single SC, an internode ranges from 200 to 2,000 μm in length (Scherer 1999). The node of Ranvier represents the region where the territories of two Schwann cells meet and is an approximately 1 μm long axon segment not covered by myelin. If viewed longitudinally, the diameter of the myelinated fiber is much the same throughout the internode, excepting some swelling at the region of the nucleus and terminally at the paranodal region (Thomas et al. 1993). The nucleus of a myelinating SC is elongated and about 50 μm long, and thus, on cross sections about 3 % of large myelinated fibers and 9 % of small myelinated fibers are cut through the SC nucleus (Ochoa and Mair 1969).

5.1.1.1 Internodal Structure of Myelinated Fibers

Cross-sectional profiles at the internode reveal a compact myelin sheath surrounded at its internal (adaxonal) and external (abaxonal) aspects by thin rims of SC cytoplasm (Fig. 5.1). Conceptually, if the spiral myelin sheet is unrolled, most of it is seen to consist of compact myelin, with inner and outer semi-compact belts which contain thin layers of Schwann cell cytoplasm. The Schwann cell nucleus, elongated parallel to the axis of the fiber and found at mid-internode, is associated with an expansion of the cytoplasm where organelles such as elongated mitochondria, endoplasmic reticulum, a Golgi apparatus, 10 nm thick filaments, microtubules, the occasional centriole, and a number of inclusions can be identified. Variable amounts of free cytoplasmic glycogen are present. The vast majority of SC organelles are concentrated in the perinuclear region. Plasmalemmal vesicles (caveolae) fuse with the outermost layer of Schwann cell membrane in regions of cytoplasmic expansion (Mugnaini et al. 1977).

The first turn of the myelin sheath overlaps itself at the inner mesaxon. A tight junction seals this site of overlap and leads into the first intraperiod line, formed by the apposition of two outer faces of Schwann cell plasma membrane. Separating the innermost aspect of the Schwann cell sheath and the axolemma is an extracellular gap with a constant width of 12–14 nm. The outer mesaxon is the site where the last turn of Schwann cell cytoplasm overlaps itself and has a tight junction just before opening up to the extracellular space. A basement membrane invariably encloses the outermost portion of Schwann cell cytoplasm. This extracellular

J.M. Bilbao, R.E. Schmidt, *Biopsy Diagnosis of Peripheral Neuropathy*,
DOI 10.1007/978-3-319-07311-8_5, © Springer International Publishing Switzerland 2015

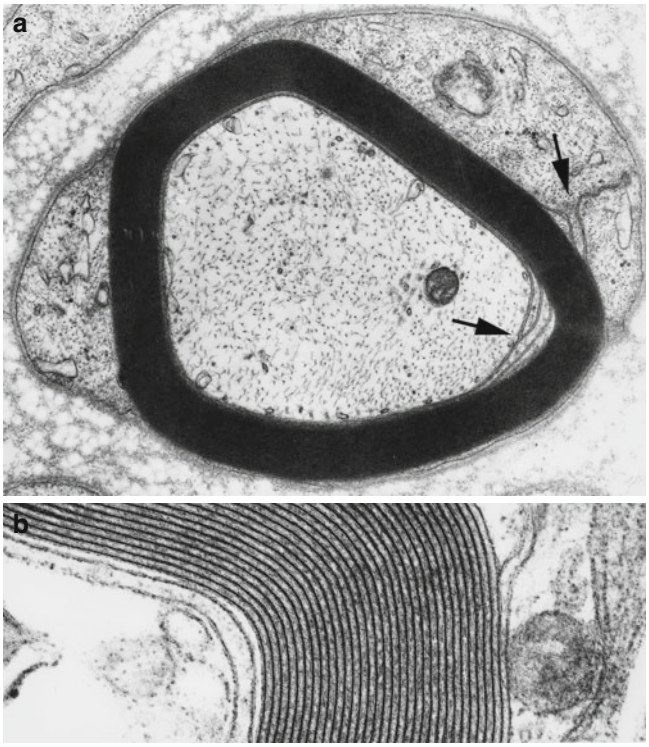

Fig. 5.1 Normal myelinated fiber. Note proximity of inner and outer mesaxons (*arrows*, **a**). High-magnification view allows resolution of the double layer of the intraperiod line (**b**) (**a** 32,200×; **b** 131,520×)

layer, composed of laminin, collagen types IV and V, heparan sulfate, and other macromolecules, forms a continuous "Schwann tube" around the nerve fiber, extending from cell body to nerve terminal (Bunge 1993). Cell culture studies have demonstrated that Schwann cells synthesize their own basement membrane (Bunge 1993).

5.1.1.2 Schmidt–Lanterman Clefts

The adaxonal and abaxonal semi-compacted and uncompacted Schwann cell cytoplasmic regions communicate through channels that run transversely across the spiraled compact myelin layers. These are the Schmidt–Lanterman (SL) clefts (Ghabriel and Allt 1981) (Figs. 5.2 and 5.3). Schmidt–Lanterman incisures are distinguished from compact myelin by the presence of Schwann cell cytoplasm (i.e., the major dense lines are not fused).

Because Schmidt–Lanterman clefts are fragile structures, a fully preserved cleft is rare in ordinary biopsy material. Typically, one sees a partial or full circumferential myelin "split" representing the disrupted SL cleft region (Fig. 7.1). When an intact SL cleft is seen in cross sections, it appears as partial or full circumferential array of stacked Schwann cell cytoplasmic pockets formed by focal separation of myelin at the major dense line (Fig. 5.2). On longitudinal cuts these pockets are revealed to be conically arranged and form an angle of about 9° to the long axis of the nerve fiber (Fig. 5.3a). The apex of the SL cleft "cone" does not point in a definite direction, and adjacent clefts may point in the same or opposite direction (Fig. 5.3a).

The linear density of SL clefts increases with the number of myelin lamellae present. In large myelinated fibers of human sural nerve, Buchthal et al. (1987) found about 35 clefts per mm, with each cleft having a length of about 13 μm. In small myelinated fibers of human sural nerve, these authors found about 8 clefts per mm of internode, each cleft measuring about 9 mm in length. Thus, with cross-sectional cuts one might expect to see clefts in about a 33–50 % of large myelinated fibers and 5–10 % of small myelinated fibers. Schmidt–Lanterman clefts can be seen in even the thinnest myelinated fibers (Hall and Williams 1970; Ghabriel and Allt 1981).

The cytoplasm within SL clefts often has a granular appearance and typically contains a single microtubule and less often membrane-bound organelles including mitochondria (Fig. 5.3). Incisure membranes are similar to paranodal loop membranes in that they lack compact myelin membrane proteins and contain myelin-associated glycoprotein (MAG). Immunohistochemical studies have shown preferential localization of connexin 32 to Schmidt–Lanterman incisures. The outermost few turns of the SL cleft may show a desmosome-like region of electron density. In addition to typical SL clefts, the myelin sheath contains some transverse cytoplasmic channels which terminate blindly and do not connect the inner and outer cytoplasmic belts. The myelin sheath also has longitudinal channels that run parallel to the axis of the nerve fiber (Mugnaini et al. 1977).

The function of SL clefts is unknown. They were previously considered by some to be artifactual, and indeed a distortion of the SL clefts is responsible for most myelin splits seen in cross sections (Fig. 7.1). However, in vivo studies conclusively prove their existence (Hall and Williams 1970). They may serve as a pathway of intracellular communication between the inner and outer Schwann cell cytoplasmic compartments. Some investigators have suggested that SL clefts give the myelin sheath a site into which newly synthesized cell membrane can be incorporated (Celio 1976) and may allow nerve fibers to tolerate bending and stretching better (Buchthal et al. 1987).

In Wallerian degeneration, early alterations occur at the SL clefts and the initial myelin ovoid consists of the myelin between two clefts (Williams and Hall 1971; Ghabriel and Allt 1979). In uncompacted myelin, a pathological alteration most often seen in paraproteinemic neuropathies with the POEMS syndrome, loss of myelin compaction, often begins at the Schmidt–Lanterman clefts; indeed it is sometimes difficult to distinguish between early loss of myelin compaction and normal variation in the form of the SL cleft (vide infra). Schroder and Himmelmann (1992) have studied pathological

Fig. 5.2 Schmidt–Lanterman incisures. Note hemidesmosome-like areas of attachment in (**a**, *arrow*). Microtubules are present in the cytoplasm of the incisures (**b**, *arrow*) (**a** 13,307×; **b** 21,888×)

alterations at the SL cleft. Their work describes described granular degeneration, vesiculation, formation of membranous whorls, and accumulation of inclusions at the SL clefts as early but nonspecific findings in neuropathy, although more often seen in demyelinating processes.

5.1.1.3 The Nodal and Paranodal Structures

The paranodal segments are 5–7.5 μm in length at either side of the internode, depending on axon diameter (Berthold and Rydmark 1983). As the fiber approaches the node (Fig. 5.4a), it loses its rounded contour and develops grooves in both the myelin and the underlying axon, creating a crenated cross-sectional appearance (Fig. 5.4b). Within each crenation are cytoplasmic accumulations of membranous organelles; mitochondria are especially numerous (Figs. 5.3b and 5.4b). The appearance of the axon at this region is described in detail in Chap. 4. Further structural and molecular details regarding nodal and paranodal organization are provided in a variety of publications (Berthold and Rydmark 1983; Salzer et al. 2008; Scherer 1999; Scherer and Wrabetz 2008; Thomas et al. 1993; Buttermore et al. 2013; Kidd et al. 2013). The last 3–5 μm of the internode is the site of myelin loop termination. Seen longitudinally, the innermost myelin lamella terminates first, as the major dense line opens up to form a small "terminal cytoplasmic pocket." This pocket attaches to the axolemma by a gap junction-like complex (Fig. 5.3b). The periaxonal space at this point of attachment measures 3–5 nm, in contrast with the 12–14 nm seen in the internodal region. The juncture of myelin loops with the underlying axolemma is a complex arrangement involving contactin, CASPR, and an isoform of neurofascin, NF155 (see Kidd et al. for review). Subsequent lamellae behave similarly, but in thickly myelinated axons there is insufficient room for all the lamellae to attach to the axons, so 80–90 % of the terminal myelin loops are coiled on top of one another in sets of 10–25, creating a picture reminiscent of "ears of barley" (Thomas et al. 1993). Junctions attach terminal myelin loops to one another and to the axolemma where possible. Freeze fracture studies reveal a complex membrane particle structure, some of which represents ion channels essential for the electrical conducting function of the axon (Wiley and Ellisman 1980).

A space of about 1 μm separates the terminal myelin loops of one paranode from those of the one opposing it. Through the center of this space runs the axon (Fig. 5.3b). Slightly overlapping extensions of the Schwann cell of each internode roof over the nodal space. These extensions project numerous radially arrayed microvilli into the nodal gap, to

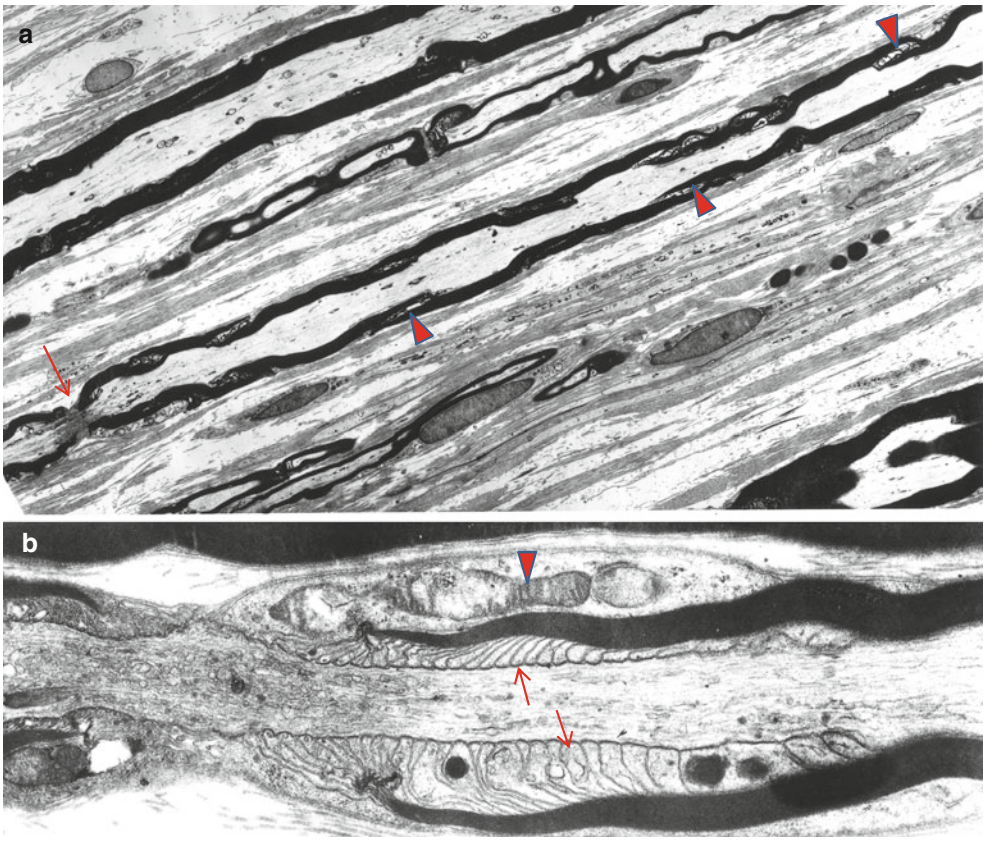

Fig. 5.3 Longitudinal view shows myelinated fibers and a node of Ranvier (*arrow*). Note that incisural cones do not have the same orientation (*arrowheads*). In (**b**) the paranodal area shows terminal cytoplasmic pockets (*arrows*) attaching to the axon and condensation of the nodal and paranodal axoplasm. The paranodal area displays a pocket of Schwann cell cytoplasm containing mitochondria (*arrowhead*) (**a** 1,450×; **b** 17,040×)

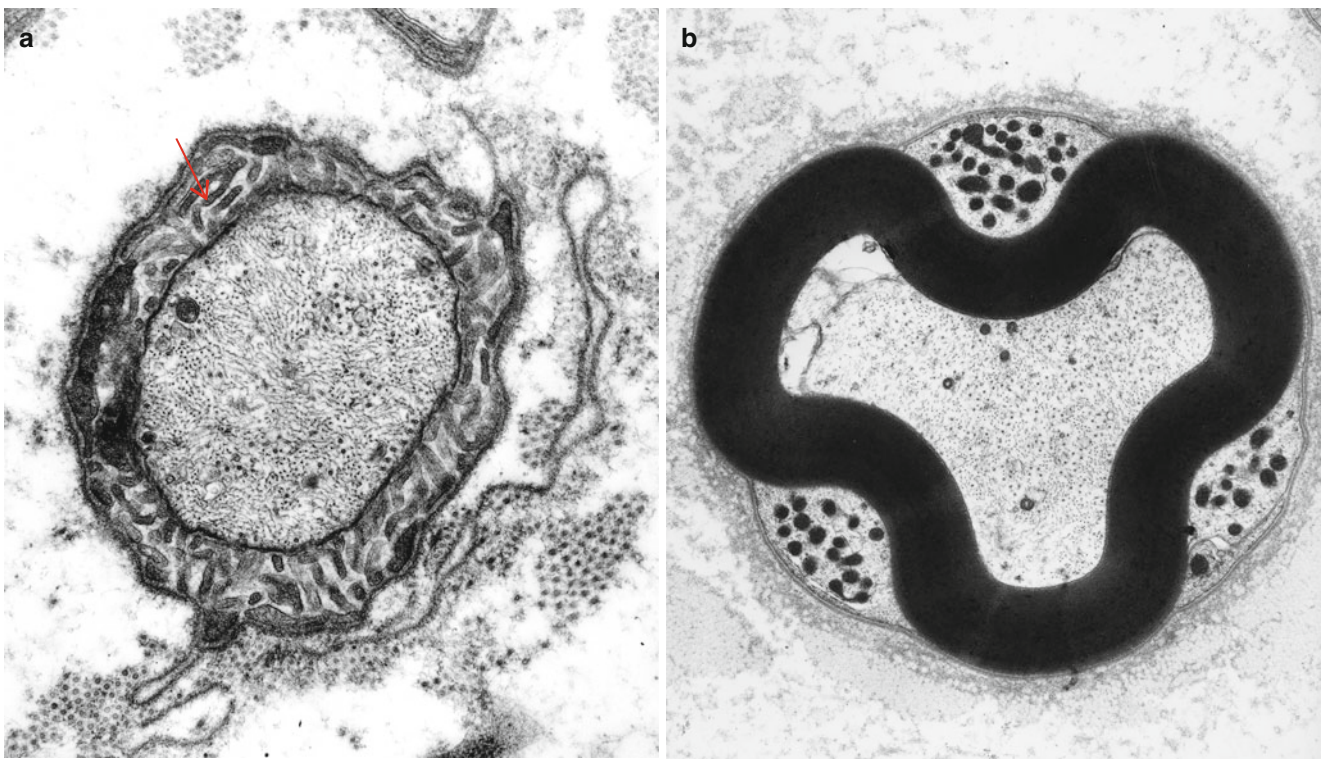

Fig. 5.4 Cross section through the node of Ranvier (**a**) and the paranodal area (**b**). In (**a**) Schwann cell microvilli (*arrow*) surround the axon. In (**b**) the crenated appearance of myelin conforms to three mitochondria containing pockets (**a** 16,302×; **b** 9,230×)

terminate within 5 nm of the axon (Fig. 5.4a). There is a gap substance around microvilli filling the space between the Schwann cell nodal processes and the basal lamina. This gap substance contains glycosaminoglycans with cation-binding and exchange properties maintaining an osmotically inactive concentration of sodium ions and limiting diffusion of K+ away from the node. The microvilli are enriched in actin filaments and actin-associated proteins. The Schwann tube (basal lamina) that surrounds all Schwann cells bridges over the nodal and paranodal structures and has equally complex constituents consisting of collagens, laminins, nidogen (entactin), fibronectin, and proteoglycans such as glypican and perlecan (Aszodi et al. 2006).

5.1.2 Myelin

Myelin is a multilamellated membranous substance produced through structural and biochemical modification of Schwann cell plasma membrane (reviewed in Webster 1993; Mezei 1993; Scherer 1999; Scherer and Wrabetz 2008; Svaren and Meijer 2008). Schematic drawings invariably illustrate mature myelin as a smooth cylindrical structure, but in reality serial sections reveal occasional infoldings and outpouchings, which in cross sections may appear as isolated "ovoids" or "loops" of myelin. Such alteration is more common in large myelinated axons, particularly near the node (Webster and Spiro 1960). The appearance can be misinterpreted as artifactual or as an indicator of pathology, as emphasized by Webster and Spiro (1960). Elzholz bodies, and myelin "wrinkling," are probably related to this myelin irregularity.

5.1.2.1 Determinants of Internode Parameters

The three principal parameters that govern conduction in a myelinated fiber are axonal diameter, myelin thickness, and internode length (Waxman 1980). Maximal internodal lengths are about 200–300 μm at birth and increase to adult values in close parallel with somatic growth (Gutrecht and Dyck 1970; Schlaepfer and Myers 1973; Friede et al. 1981). The actual site of a node of Ranvier is determined prior to the onset of myelination by specializations of the axolemma which presumably interact with the Schwann cell to limit its longitudinal growth (Wiley-Livingston and Ellisman 1980; Waxman 1980). Somatic elongation from onset of myelination to adult life is the main factor governing internode length (Friede et al. 1981). Larger-diameter axons have longer internodes, perhaps because these fibers myelinate earlier and are thus subject to a relatively greater degree of somatic growth (Thomas and Young 1949; Schlaepfer and Myers 1973). However, this explanation is incomplete, as the total complement of large and small myelinated fibers in human nerve is probably obtained very early in life (Jacobs 1988).

Myelin thickness is proportional to axon diameter, and in a first approximation, a single linear relationship provides a good degree of correlation across all fiber sizes (Behse 1990). However, small myelinated fibers are relatively more thickly myelinated than large myelinated fibers (Behse 1990; Friede and Bischhausen 1982). For axons of a given diameter, myelin thickness seems to increase slightly with internode length, a finding that is congruent with theoretical considerations (Friede and Bischhausen 1982; Friede and Beuche 1985).

5.1.2.2 The Structure of Compact Myelin

The periodicity of compact PNS myelin in vivo is 18 nm, although fixation usually reduces this to 15 nm, mostly through dehydration (Kirshner and Ganser 1984). The major dense line is about 6 nm thick and is made up of the fused cytoplasmic aspects of the Schwann cell membrane. In vivo the major dense line is actually composed of two membrane leaflets separated by about 2 nm of intracellular space. However, glutaraldehyde fixation and osmium tetroxide postfixation remove water and some membrane lipids, resulting in fusion of the two layers (Kirshner and Ganser 1984). The intraperiod line (IPL) is made up of two thinner lines, each representing the outer leaf of the Schwann cell plasma membrane, separated by about 4 nm (Fig. 5.1b). Thus, the region between the two leaves of the IPL is contiguous with the extracellular environment, and the space within the major dense line (in vivo) is contiguous with the Schwann cell cytoplasm.

Although the space within the IPL is contiguous with the extracellular matrix, junctional complexes at the outer and inner mesaxons and at the nodal area somewhat restrict flow of molecules and ions in this space (Chernousov et al. 2008). Because the cell membranes lining the IPL space have a negative charge (Inouye and Kirschner 1988), cations find their way into it more readily than anions or neutral molecules (Ropte et al. 1990). The presence of cations within this space is important for maintenance of the normal periodicity, as removal of positive charges results in widening of the space, presumably due to repulsion from unmasked opposing negative charges (Ropte et al. 1990).

5.1.2.3 Composition of Myelin

Myelin is a modification of the Schwann cell membrane. It contains 45 % water by weight, and the composition of dehydrated human myelin is 71 % lipid and 29 % protein (Inouye and Kirschner 1988; Norton and Cammer 1984). The important lipid components are phospholipids (55 % of total lipids), glycolipids (cerebrosides, sulfatides, and gangliosides representing 22 % of total lipid), and cholesterol (23 % of total lipid). Physiologically and clinically important proteins include P_0, P_1, and P_2 glycoproteins, peripheral myelin protein (PMP)-22, and myelin-associated glycoprotein (MAG).

Glycolipids occur only on the external layer of the Schwann cell membrane and thus are localized to the

intraperiod line (Inouye and Kirschner 1988). Immunization of experimental animals with galactosylceramide can produce experimental allergic neuritis (EAN), an animal model for Guillain–Barré syndrome (Stoll et al. 1986). Monoclonal and polyclonal antibodies to gangliosides have been identified as potential causative agents of human demyelinating and axonal neuropathies. Metachromatic leukodystrophy and Krabbe leukodystrophy are inherited diseases with defects in glycolipid metabolism which produce a demyelinating neuropathy, although the mechanism of the neuropathy is uncertain.

P_0 is a 30 kDa transmembrane glycoprotein which makes up about 60 % of all PNS myelin protein by weight, but is not present in CNS myelin or in nonmyelinating Schwann cells (Giese et al. 1992). It may function in maintaining the compaction of myelin at both the intraperiod and major dense lines (Lemke et al. 1988; Filbin and Tennekoon 1991). Immunization with P_0 protein can produce EAN (Milner et al. 1989), and antibody against P_0 protein has been associated with a severe childhood hypertrophic neuropathy (Ben Jelloun-Dellagi et al. 1992). Mice with defective P_0 protein expression show loss of most myelin compaction. However, some degree of myelin organization remains, indicating that proteins other than P_0 are important in this role (Giese et al. 1992). Mutations in P_0 protein have been implicated in the human familial neuropathies CMT-1B and Dejerine–Sottas syndrome (CMT-3).

P_1 protein (identical to CNS myelin basic protein) has been extensively studied in its role as the major neuritogenic antigen of experimental allergic encephalitis (Linington and Brostoff 1993). This is a glycoprotein with multiple isoforms, of which the 18 kDa variant is the most important. It accounts for a species variable 2–16 % of PNS protein. P_1 is found on the cytoplasmic aspect of the Schwann cell membrane, but its function in PNS myelin is largely unknown (Linington and Brostoff 1993; Peterson and Bray 1984).

P_2 is a 14.8 kDa glycoprotein found predominantly in the PNS where it makes up 2–15 % of myelin protein (Linington and Brostoff 1993). It is located in the cytoplasmic layer of Schwann cell membrane, particularly in regions where myelin is not compacted (Trapp et al. 1979). The physiologic function of P_2 protein is uncertain. P_2 glycoprotein is the major antigenic stimulus for production of EAN by immunization with peripheral nerve myelin (Rostami 1993).

Peripheral myelin protein-22 (PMP-22) is a more recently discovered 18 kDa integral membrane protein found primarily in PNS myelin (Suter et al. 1993). Although it is localized to compact myelin, its physiologic importance is unknown. Mutations in the PMP-22 gene in mice produce the Trembler phenotype. In humans, there is a strong association between defects involving the PMP-22 gene and CMT-1A hypertrophic neuropathy as well as hereditary neuropathy with liability to pressure palsies (HNPP).

Myelin-associated glycoprotein (MAG) is a 100 kDa transmembrane protein found in both the CNS and the PNS. This protein has an immunoglobulin-like domain on the outer face of the Schwann cell/oligodendrocyte membrane. Quantitatively, it makes up only 0.1 % of PNS myelin protein (Trapp 1990). In PNS myelin, MAG is found in the periaxonal space, paranodal regions, Schmidt–Lanterman clefts, and inner and outer mesaxonal membranes (Trapp 1990; Kidd et al. 2013). All membranes containing MAG appose other membranes by 12–14 nm (Trapp 1990). MAG is a member of the family of cell adhesion molecules and may play a role in maintaining the anatomical and physiologic integrity of the myelin sheath–axon unit. It may also be important in initiating the process of myelin formation and in controlling which parts of the Schwann cell cytoplasm become compacted (Leblanc and Poduslo 1990; Trapp 1990). IgM paraproteins with specificity against MAG have been strongly implicated in the causation of a common human demyelinating neuropathy.

5.1.3 Nonmyelinating Schwann cells

In humans sural nerve nuclear counts show that nonmyelinating Schwann cells (NMSCs) outnumber myelinating SCs by a factor of 4:1 (Ochoa and Mair 1969). Significant differences exist in the biology of nonmyelinating Schwann cells compared to myelinating Schwann cells (reviewed in detail by Griffin and Thompson 2008). In contrast to the strict 1:1 relationship between axons and Schwann cells seen in myelinated fibers, single or multiple NMSC profiles may be seen without associated axons, or a single NMSC may be seen to support one, two, or more axons. A Schwann cell subunit (ScSu) has been defined as any single Schwann cell profile or group of profiles that in cross section is enclosed by a continuous basal lamina (Sharma and Thomas 1975). Schwann cells surrounding a collection of unmyelinated axons have been designated as Remak fibers, a term which refers only to unmyelinated fibers. Remak Schwann cells have territories that extend longitudinally for 50–100 μm and ensheathe different axon modalities. Unmyelinated axons exchange frequently among different Remak bundles during their proximodistal courses (Kidd et al. 2013). Quantitative aspects of Schwann cell subunits are reviewed elsewhere. The discussion here will focus on ultrastructural features.

Schwann cell cytoplasm completely encircles most unmyelinated axons, although occasionally one may see a segment of axon that is in direct contact with the surrounding basement membrane. The formation of individual mesaxons for each unmyelinated axon is thought to be the result of secretion of neuregulin 1 type III (Taveggia et al. 2005). Nonmyelinating Schwann cell cytoplasm contains

the same complement of organelles as myelinating Schwann cells. The NMSC nucleus is elongated, 10–20 μm long, with only about 1 in 14 Schwann cell profiles showing the nucleus in cross section (Carlsen et al. 1974); the typical length of an NMSC has been estimated at 200–500 μm (Carlsen et al. 1974).

It may be difficult or impossible to distinguish a circular NMSC profile from an axon when the cross section contains no nucleus. Some criteria assist in making the distinction (Dyck 1969; Gibbels 1989). Axons are more likely to be round and tend to be less electron dense than Schwann cell processes. Neurofilaments and neurotubules are found in roughly equivalent numbers in unmyelinated axons, but tubules are far less prominent than filaments in Schwann cells. The formation of a mesaxon around a circular profile favors the possibility that the circular profile is an axon. The axolemma tends to have a greater electron density than the Schwann cell plasma membrane.

Occasionally, several Schwann cell processes may surround an axon. This occurrence usually relates to regions where the longitudinal extent of one Schwann cell ends and the next begins. These junctional points are not as clearly demarcated as the nodes of Ranvier in myelinated fibers. Studies by Eames and Gamble (1970) demonstrate how Schwann cell processes form variably complex regions of overlap and interdigitation at the junction point. Often the cytoplasm of the innermost Schwann cell at the site of overlap is particularly electron dense (Eames and Gamble 1970). Bundles of collagen may be partially or fully encircled by Schwann cell cytoplasm. These "collagen pockets" (Fig. 2.12) increase in prominence with age and in neuropathy. Denervated ScSus are identified by their lack of axons. This condition also occurs in normals, but increases with age or pathology.

5.1.3.1 Control of Myelination Phenotype

Myelination requires a balance of transcriptional programs (reviewed in Mirsky et al. 2008) with positive regulators of this process, including Krox-20, Sox-10, and Oct-6, and negative regulators (Notch, Sox-2, Pax-3, Id2, Krox-24, and Egr-3) which are expressed prior to myelination, downregulated as myelination starts, and reactivated as Schwann cells dedifferentiate following injury which is required for effective nerve regeneration.

5.1.4 Schwann Cell Inclusions

5.1.4.1 Reich Pi Granules

These inclusion bodies are typically found adjacent to the nucleus of myelinating Schwann cells (arrows, Fig. 5.5a, b). They can be seen by light microscopy and may number in the dozens within a perinuclear region (Fig. 5.6a, b). Reich identified their metachromasia with aniline dyes and noted that they had different staining properties than mast cell granules – a point of controversy at the time (Reich 1903). Pi granules are metachromatic with toluidine blue (Fig. 5.5a), Hirsch–Peiffer, and methylene blue stains, are refractile under polarized light (Fig. 5.5b), and will stain positively with Sudan black and PAS on frozen material (Noback 1953; Olsson and Sourander 1969). Their positive staining for acid phosphatase identifies them as lysosomes (Weller and Herzog 1970). Pi granules are best seen with the electron microscope, where they appear as single membrane-bound organelles, typically 1 μm in size, whose contents are often partially or totally removed in processing. However, when a structure can be discerned, there is usually a lamellar pattern with a periodicity less than that of myelin (5 nm vs. 12–17 nm) (Fig. 5.6b). At time they may take a "zebra body"-like appearance or contain globules of amorphous variably osmiophilic material. Their shape may be elongated, oval, or polygonal. In nerves undergoing active degeneration, we have seen pi granule-like inclusions within macrophages, perhaps representing the indigestible remains of Schwann cells. Thomas et al. (1993) have indicated that pi granules are not found in nonmyelinating Schwann cells. Although pi granule-like inclusions can rarely be seen in NMSCs, such configurations may represent denervated, formerly myelinating, Schwann cells.

Reich pi granules normally appear in myelinating Schwann cells, but are mostly restricted to the perinuclear area, so most fibers seen in cross sections do not show them. Rarely, they can be encountered in the paranodal Schwann cell cytoplasm. They are said to not be present in nerves of young people (<8 years of age, Robson 1951); Reich himself (1903) pointed out that the inclusions were not seen in the first years of life. Most authors have indicated, without formal quantitation, that pi granule numbers increase with age, suggesting that they are a "wear-and-tear"-related accumulation (Babel et al. 1970, p 48; Weller and Herzog 1970; Leibowitz et al. 1983; Asbury and Johnson 1978; Thomas et al. 1980; Robson 1951). It is noteworthy that they are not seen in recently remyelinated fibers (Weller and Herzog 1970).

Pi granules can be more prominent in neuropathy (Evans et al. 1965; Dyck and Lambert 1970; Shetty et al. 1988), but this is nonspecific. They may also be seen in increased numbers in some storage diseases (Goebel et al. 1976), but workers should exercise care not to confuse them with zebra bodies or other abnormal storage material (Olsson and Sourander 1969).

No major advances in the understanding of the nature of pi granules have taken place since Noback provided histochemical evidence for earlier suggestions that the granules were composed of sulfatides and/or phosphatides in the 1950s (Noback 1953, 1954).

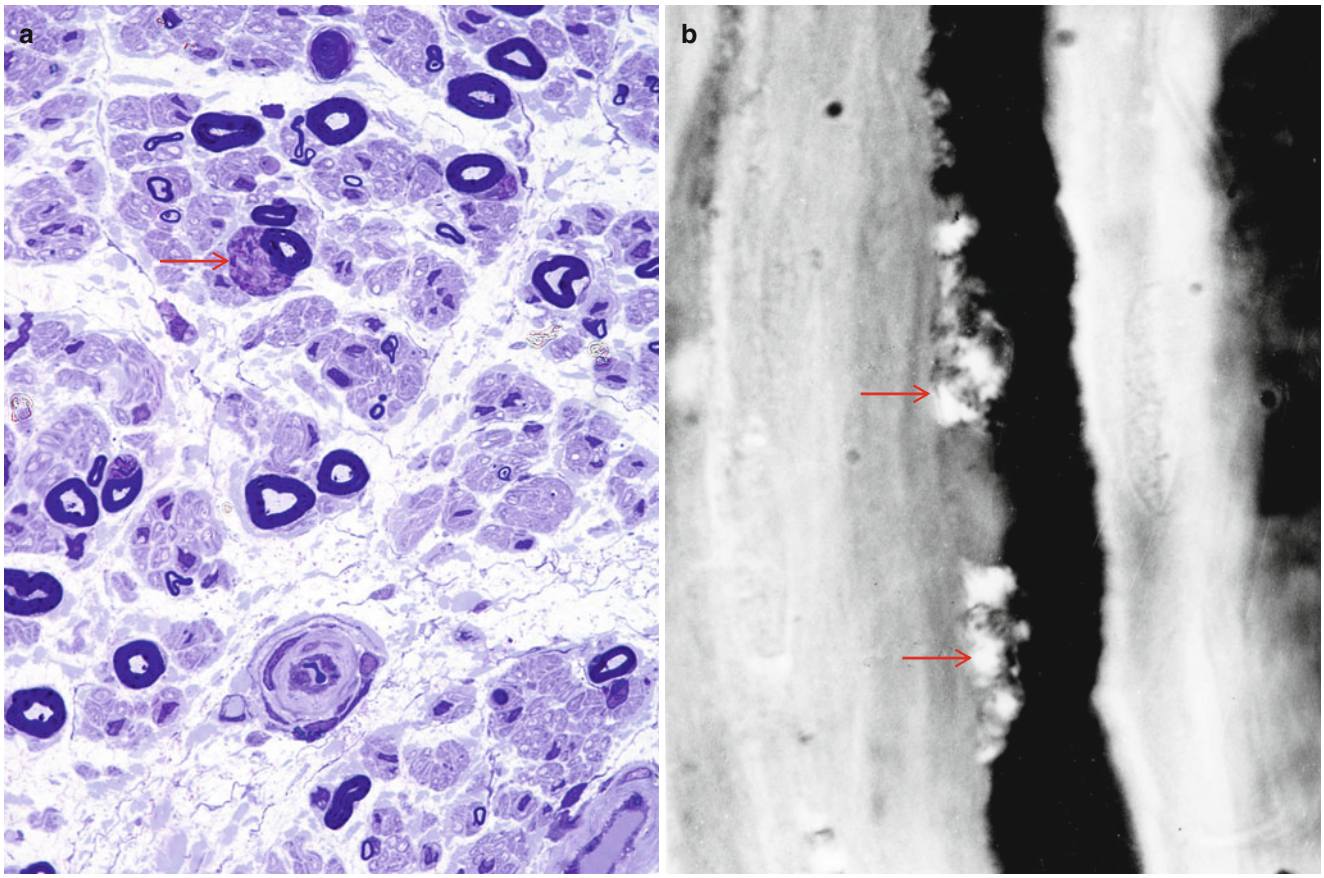

Fig. 5.5 Reich pi granules. These osmiophilic and metachromatic structures (*arrow*, **a**) are usually found in the perinuclear Schwann cell cytoplasm. In (**b**) a teased fiber preparation demonstrates refractile pi bodies (*arrows*) adjacent to the nucleus (**a** 1 μ plastic, 1,000×; **b** teased fiber photographed under half-crossed polarizing filters)

5.1.4.2 Elzholz Bodies (Mu Granules)

Elzholz bodies are rounded, osmiophilic, Marchi-positive bodies containing unsaturated lipid seen in the cytoplasm of myelinating Schwann cells, external to compact myelin, and most frequently in the perinuclear and paranodal regions (Schroder and Himmelmann 1992; Dyck et al. 1984a) (Fig. 5.7). Electron microscopy reveals a periodicity similar to that of myelin. No pathological significance has been attached to Elzholz bodies, and they may be seen in normal nerves. Most likely their formation is related to myelin remodeling and to the loops and redundant myelin folds that are seen in normal and abnormal myelinated fibers (Webster and Spiro 1960; Schroder and Himmelmann 1992).

5.1.4.3 Lipofuscin

Lipofuscin is an insoluble intracellular pigmentary accumulation seen in a variety of tissues throughout the body. Intracellular storage of lipofuscin results from the gradual accumulation of indigestible residues of autophagy and likely reflects the "wear and tear" of aging. In the PNS, the main site of accumulation of lipofuscin is in nonmyelinating Schwann cells, where the substance appears as autofluorescent single membrane-bound material, most of which is electron-dense amorphous or granular, intermingled with lightly or moderately electron-dense lipid droplets (Fig. 5.8). In one study the number of lipofuscin granules increased by a factor of 4 from age 17 to age 69 in unmyelinated fibers of human vagus nerves (Sharma and Thomas 1975). Although lipofuscin is normally not demonstrable in myelinating Schwann cells (Thomas 1993), such occurrence has been noted in Refsum disease (Thomas 1993), adrenoleukodystrophy, and Niemann–Pick disease. We have also examined a biopsy from a patient with Dejerine–Sottas syndrome in which myelinating Schwann cells contained abundant lipofuscin.

5.1.4.4 Other Inclusions

Some Schwann cell inclusions are of great value in the diagnosis of storage diseases and certain intoxications; these are discussed elsewhere (Table 7.9; Chap. 20). Other dense membrane-bound

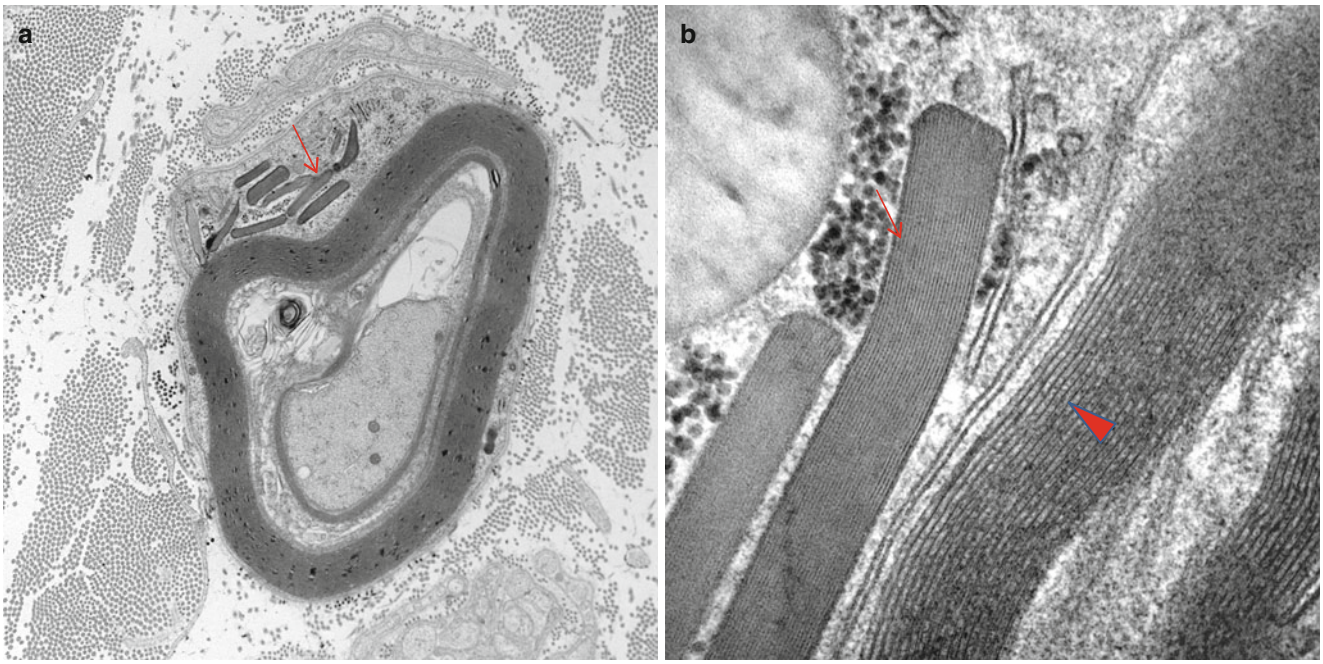

Fig. 5.6 Reich pi granules. Membrane-bound pleomorphic inclusions of variable osmiophilia are seen in the perinuclear region. Some rodlike granules (*arrow*, **a**) have a fine periodicity different from adjacent myelin (*arrowhead*, **b**) (**a** 12,000×; **b** 100,000×)

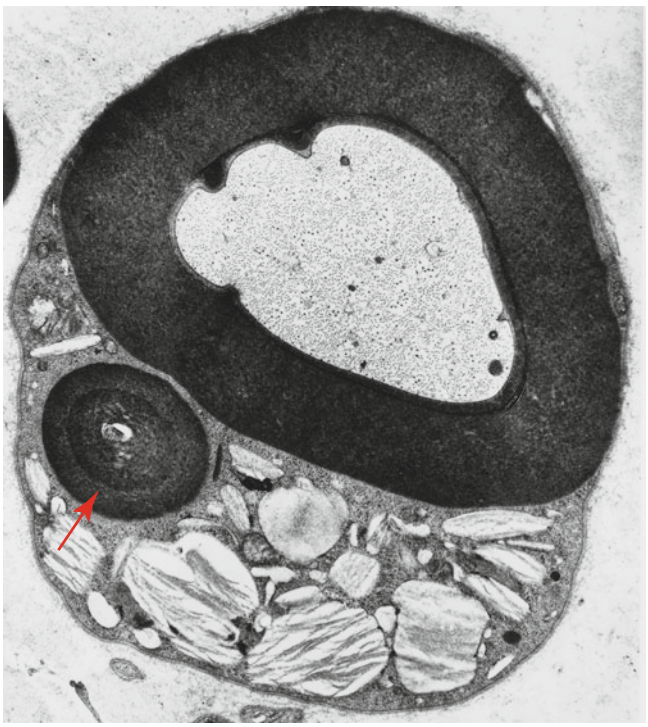

Fig. 5.7 Elzholz body. In contrast to pi bodies, the Elzholz body (*arrow*) is rounded and has the periodicity of myelin (11,400×)

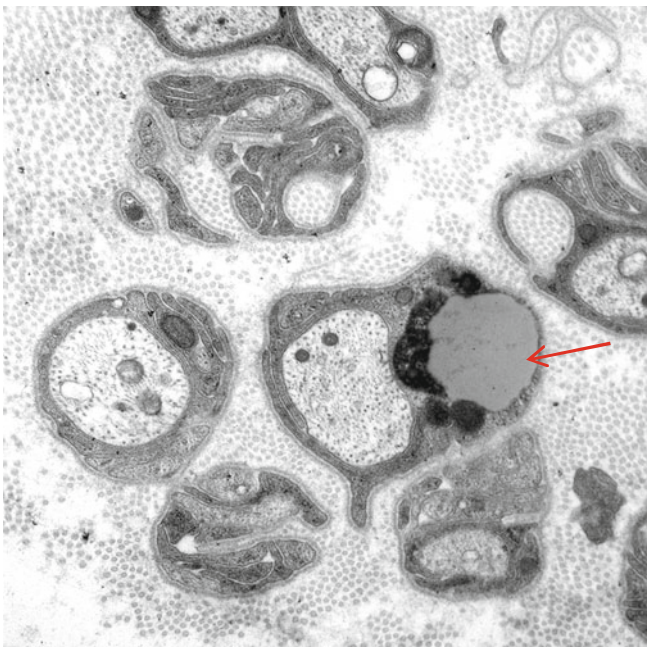

Fig. 5.8 Schwann cell inclusions. Lipofuscin (*arrow*) is ordinarily only found in nonmyelinating Schwann cells (magnification, **a** 20,235×; **b** 8,915×)

inclusions of uncertain significance may be seen in Schwann cells. Some of these probably would have been identified as "Elzholz bodies" by some workers. Osmiophilic inclusions seem to be more numerous in "sick" or stressed Schwann cells and probably represent autophagic vacuoles. Glycogen accumulation in the occasional myelinating and nonmyelinating Schwann cell can be striking, but is nonspecific. Increased Schwann cell glycogen may be particularly prominent in glycogenoses and hypothyroidism (Dyck and Lambert 1970).

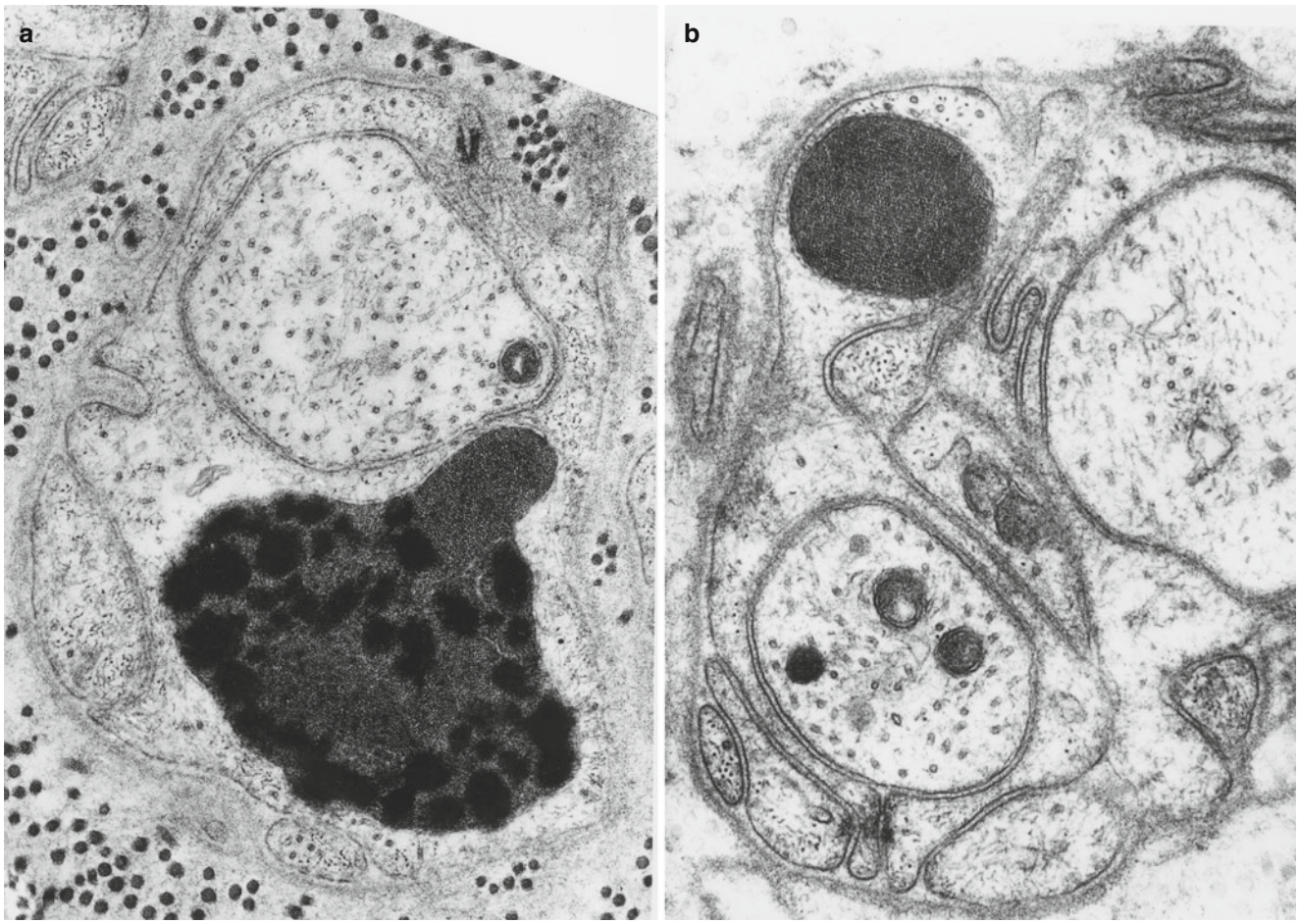

Fig. 5.9 Schwann cell inclusions. Paracrystalline inclusions are not uncommon in chronic neuropathies. These are probably of mitochondrial origin and may contain lipid (**a** 34,884×; **b** 35,700×)

One may observe double membrane-bound paracrystalline inclusions with small amorphous electron-dense regions in nonmyelinating Schwann cells (Fig. 5.9a, b). Such inclusions were initially emphasized in Refsum disease in which the authors hypothesized that they might be modified mitochondria (Fardeau and Engel 1969). Subsequently, workers identified similar inclusions in a host of toxic, metabolic, and genetically based neuropathies (Thomas and King 1974; Lyon and Evrard 1970; Vallat et al. 1973; Schroder and Sommer 1991). These inclusions have no diagnostic specificity and were found in 25 of 280 unselected peripheral neuropathies, in up to 10 % of NMSC mitochondria (Schroder and Sommer 1991). We have observed such inclusions in situations including CIDP, sarcoid neuropathy, disulfiram neuropathy, diabetic neuropathy, idiopathic axonal neuropathies, and a nerve showing only minimal changes attributable to aging. Similar inclusions have also been emphasized in mitochondrial diseases (Yiannikas et al. 1986; Schroder and Sommer 1991), may be very prominent in a variety of cell types in amiodarone neuropathy, and can be produced experimentally by treating rats with inhibitors of cholesterol synthesis (Hedley-White 1973; Suzuki and DePaul 1972).

5.2 Demyelination

When studying the pathology of a neuropathic disease, one must decide whether the process is fundamentally axonal or demyelinating, as this is of great diagnostic and prognostic importance. The distinction may not be obvious, as the Schwann cell and axon are highly interdependent; a diseased axon results in disturbance of Schwann cell metabolism and myelin structure, and myelin alterations affect axon morphology. Processes involving the nerve (toxins, trauma, ischemia, inflammation) seldom damage only myelin or only the axon.

Demyelination may occur as a consequence of Schwann cell or myelin defects, in which case it is primary demyelination. However, the typical changes of demyelination can also be seen in diseases known to primarily act upon the axon. This is termed secondary demyelination. Primary demyelination may be a consequence of Schwann cell dysmetabolism with loss of ability to maintain the myelin sheath or may result from direct attack on myelin itself. The processes leading to myelin damage are many, but often the appearance of the resultant demyelination is

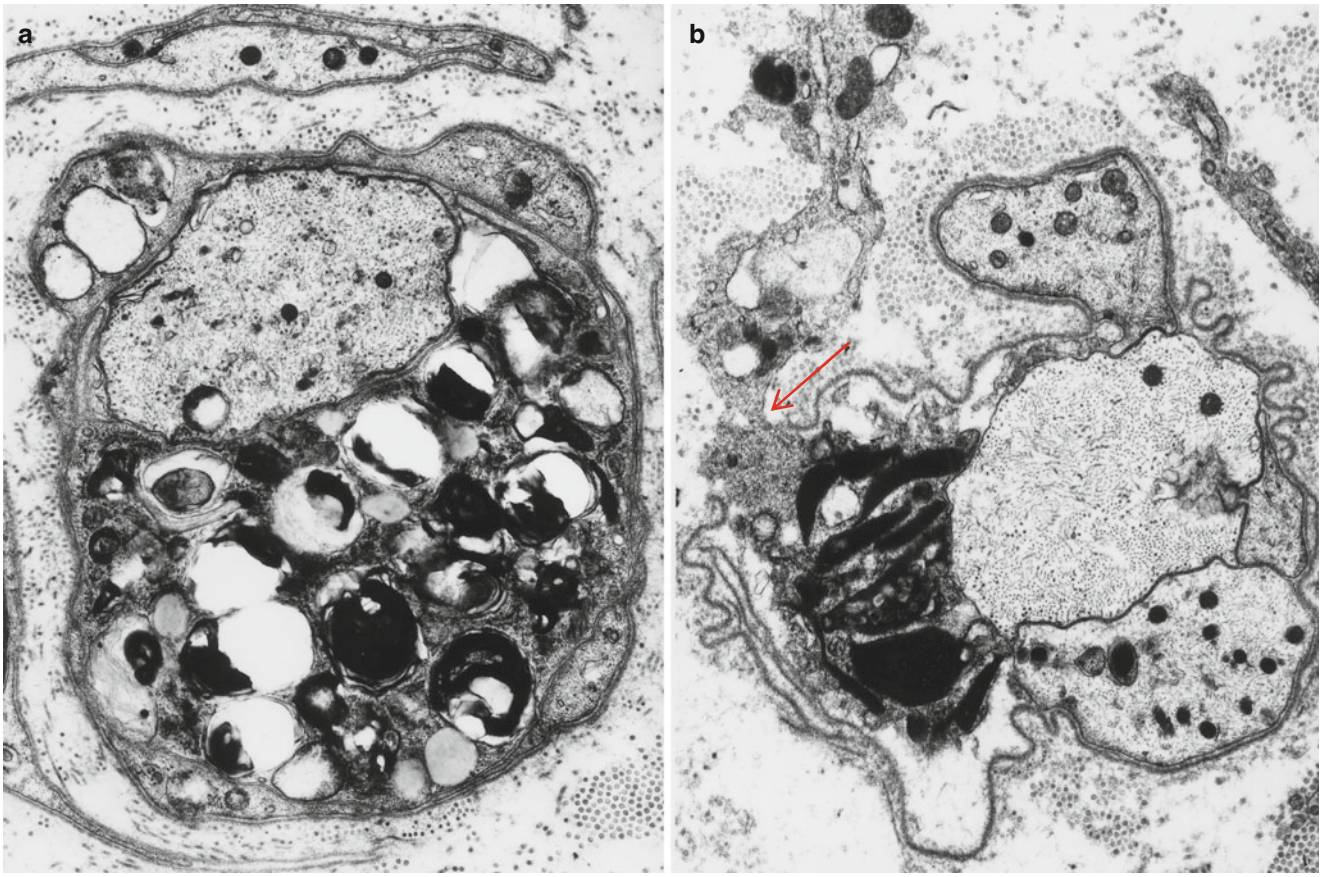

Fig. 5.10 Demyelination. In (**a**) only one of the intratubal cell processes contains debris and likely belongs to a macrophage. In (**b**) a macrophage process is captured exiting through a wide gap in the basal lamina (*arrow*) (**a** 13,760×; **b** 12,070×)

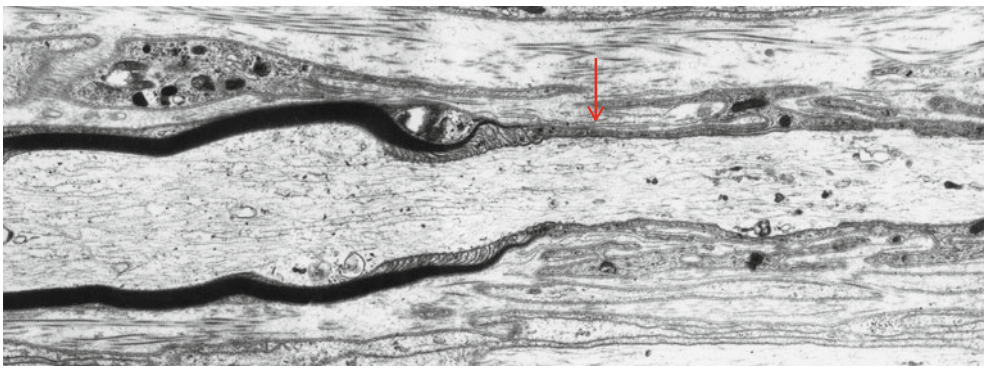

Fig. 5.11 Demyelination. Note interface (*arrow*) between remyelinated internode and a demyelinated axon (7,800×)

nonspecific. Below, we review both nonspecific and specific features of demyelination with emphasis on elements of differential diagnosis.

5.2.1 Nonspecific Features of Demyelination

A normal large diameter axon either surrounded by degenerating myelin or entirely denuded constitutes clear-cut light microscopic evidence of ongoing demyelination (Figs. 5.10a, b and 5.11). Myelin debris, consisting of osmiophilic material contained in cells around the axon or elsewhere in the endoneurium, indicates that the process is actively proceeding, as exogenous phagocytes clear debris within days to weeks. Although Schwann cells are capable of taking up myelin debris in nonphysiologic situations, they seem to leave this task to macrophages in vivo (Friede and Bruch 1993; Griffin et al. 1993).

Early myelin changes can include splitting or vacuolation of the compact myelin sheath, focal areas of vesicular

degeneration, and the appearance of myeloid bodies in Schwann cell cytoplasm. Alterations in terminal myelin loops at the node of Ranvier, small myelin "ovoids" in the paranodal regions, vesicular degeneration, and retraction of Schwann cell processes with resultant widening of the nodal gap are considered early changes in demyelination of all varieties (Asbury et al. 1969, 1978; Lampert and Schochet 1968; Masurovsky et al. 1967; Allt 1983), including that secondary to axonal disease (Dyck et al. 1981), and in axonal degeneration (Ballin and Thomas 1969a). Thus, paranodal myelin alterations should not be interpreted as evidence of a primary demyelinating process.

While a degenerating or absent myelin sheath around an intact formerly myelinated axon directly indicates demyelination, a thinly myelinated axon is a sign of remyelination. The hallmark of recurrent demyelination and remyelination is onion-bulb formation, consisting of a central axon (myelinated or otherwise) surrounded by concentric attenuated Schwann cell lamellae. Onion bulbs are described and illustrated elsewhere, and remyelination is considered below.

Buckling and splitting of myelin, inpouching and outpouching of myelin folds, and focal separation of the axon from its myelin sheath are commonly observed in nerve biopsies. Such changes can be seen in otherwise normal nerves but are clearly more prominent in neuropathy and correspond to myelin "wrinkling" seen on teased fibers (Dyck et al. 1971, 1984b; Webster and Spiro 1960). This alteration increases in frequency with the normal aging process (Dyck et al. 1993, Table 30.4) and is particularly common with myelin remodeling in response to axonal atrophy (Dyck et al. 1984b). Mechanical or chemical trauma during the biopsy procedure might also produce some of these alterations.

5.2.2 Specific Myelin Changes in Primary Demyelinating Neuropathies

5.2.2.1 Macrophage-Mediated Myelin Stripping

Destructive stripping of myelin by macrophages is the central mechanism of demyelination in the inflammatory demyelinating neuropathies, GBS and CIDP, and is generally regarded as specific to these entities (Prineas 1981; Brechenmacher et al. 1987). The macrophage penetrates the Schwann cell basement membrane and the cell membrane, separates Schwann cell cytoplasm from its myelin, and insinuates cytoplasmic fingers into the intraperiod lines of the myelin sheath. Most often this occurs in idiopathic CIDP and GBS; however, macrophage-mediated demyelination is also seen when these clinical syndromes occur in the setting of other illnesses, such as HIV infection (Cornblath et al. 1987), a circulating IgG (Pollard et al. 1983; Bleasel et al. 1993) or IgM (Vital et al. 1991) paraprotein, or lymphoma (Sumi et al. 1983). Macrophage-mediated demyelination is seen in EAN, the animal model of GBS (Wisniewski et al. 1969), and several other veterinary diseases (Marek's disease, coonhound paralysis). It also appears in recurrent lysophosphatidylcholine-induced demyelination, probably as a consequence of "self-immunization" against myelin following repeated episodes of iatrogenic demyelination (Hall 1984). Macrophage-mediated myelin stripping has rarely been described in familial hypertrophic neuropathy (Vital et al. 1992; Madrid et al. 1977) or uremia (Said et al. 1983), but we have never observed this and find the illustrative figures to be unconvincing, perhaps simply showing scavenger macrophages which have entered the Schwann tube to clear out degenerating myelin. An alternative interpretation is that these cases represent instances of inflammatory demyelinating neuropathy superimposed on another neuropathy.

Macrophage-mediated demyelination is likely the final common pathway of a variety of dysimmune phenomena. Complement and immunoglobulin deposits have been found on the Schwann cell membrane in a variety of inflammatory neuropathies (Hays et al. 1988). In theory, these substances can opsonize myelin and promote phagocytosis via the immunoglobulin and complement receptors normally found on macrophages (Stoll et al. 1991). Indeed, intact myelin seemed to be taken into coated pits in a study of inflammatory demyelination in the CNS (Epstein et al. 1983), and this process may be initiated by IgG binding to the myelin sheath (Wayne Moore and Raine 1988). However, the finding of myelin-binding antibodies or complement has been inconsistent in both CIDP and GBS (see discussion Chap. 9), and these deposits may be an epiphenomenon relating to the alteration in vascular permeability often seen early in the course of inflammatory neuropathy.

Investigators generally regard the insertion of cell processes and removal of myelin debris as discussed above and in more detail elsewhere as unique to macrophages. However, Schwann cells of unmyelinated fibers displayed identical behavior when serum from GBS patients was introduced into a neural cell culture line in a macrophage-free medium (Birchem et al. 1987). There are also reports of malignant lymphocytes in CLL apparently carrying out myelin stripping (Vital et al. 1975; Sumi et al. 1983).

5.2.2.2 Vesicular Demyelination

Myelin can sometimes disintegrate around an apparently intact axon through splitting at the major dense line, creating a netlike pattern of vesicles 80 nm in diameter (see Fig. 7.4a–c) (Arnason and Soliven 1993; Brechenmacher et al. 1987). In a different plane of section, these are seen as parallel lines, suggesting that in three dimensions the structure is composed of parallel cylinders (Carpenter 1972). Detached pieces of vesicular myelin are often seen as debris within

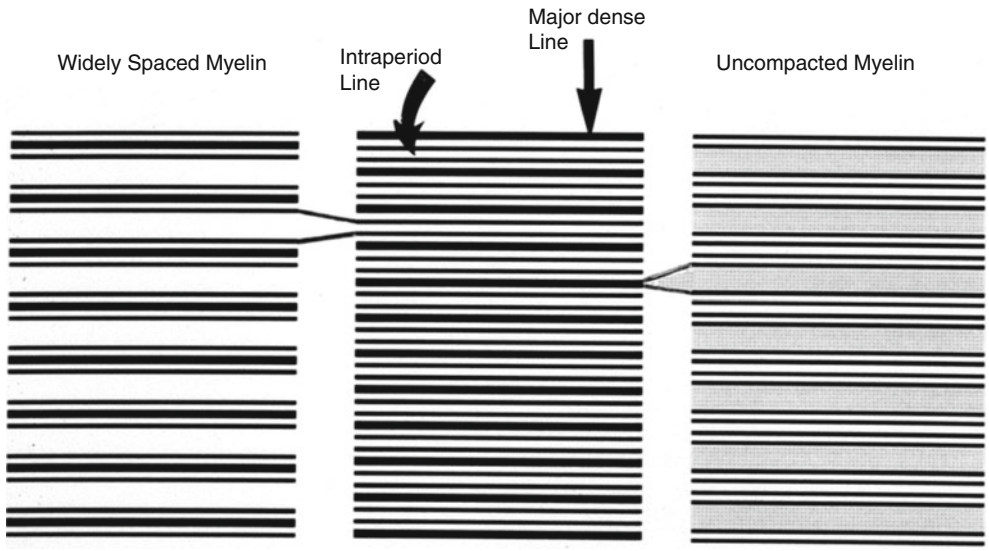

Fig. 5.12 Alterations in myelin periodicity. Widely spaced myelin (*left*) is formed by separation at the intraperiod line (*curved arrow*), while uncompacted myelin (*right*) results from separation at the major dense line (*arrow*)

macrophages. Some have noted a close correlation of this change with the postmortem state or have found similar alterations in control autopsy nerves. These workers consequently dismiss this change as an artifact of delayed fixation (Honavar et al. 1991). Indeed, in GBS there is a tendency for this finding to be reported on autopsy studies. However, vesicular demyelination has also been observed in nerve biopsy specimens (Brechenmacher et al. 1987; Vital et al. 1985; Prineas 1972; Sumi et al. 1983). Although our experience confirms that this alteration is most often an artifact of delayed fixation or accompanying crush artifact, we have observed a number of examples in well-preserved nerve biopsy material, usually in diabetic neuropathy. Injecting sera from GBS patients into nerve culture or animal peripheral nerve produces vesicular demyelination (Hirano et al. 1971; Birchem et al. 1987; Saida et al. 1982; Brown et al. 1987). In some experimental allergic neuritis (EAN) models, vesicular demyelination takes place in close association with macrophage invasion (Dal Canto et al. 1975) or prior to the appearance of any inflammatory cells (Rosen et al. 1990). The latter authors offered the hypothesis that vesicular myelin degeneration is produced by humoral factors, most likely antibodies to myelin antigens, whereas cell-mediated immunity was involved in macrophage-mediated myelin stripping (Rosen et al. 1990). Vesicular demyelination has also been observed in experimental situations where immune attack does not operate, such as lead (Lampert and Schochet 1968) or tellurium (Lampert and Garrett 1971) toxicity and radiation injury (Masurovsky et al. 1967). Incubating peripheral nerve with calcium and a calcium ionophore results in the rapid occurrence of severe diffuse vesicular demyelination without axonal damage (Smith and Hall 1988), suggesting that vesicular myelin disintegration is a nonspecific consequence of any process that causes calcium leakage into the Schwann cell, with subsequent activation of endogenous phospholipase A_2 (Smith and Hall 1988).

5.2.2.3 Abnormal Periodicity of Myelin

As discussed above, normal myelin periodicity is 18 nm in the fresh state and 12–17 nm in fixed nerves. Some peripheral nerve diseases and experimentally induced nerve lesions demonstrate regularly increase myelin periodicity. King and Thomas (1984) emphasized the importance of distinguishing between uncompacted myelin (UCM) and widely spaced myelin (WSM) (Fig. 5.12). Both these alterations are rare, but when detected have important diagnostic implications.

Uncompacted Myelin

In uncompacted myelin (UCM), the cytoplasmic aspects of the Schwann cell membrane fail to appose, leaving considerable quantities of cytoplasm between the two halves of the major dense line (Fig. 5.13a, b). Often the outer faces of the Schwann cell membrane also fail to appose, and the intraperiod line fails to form. This pathological alteration occurs in several human neuropathies and experimental models (Table 5.1), most immune related. Membranous whorled bodies can be seen within the cytoplasm at the site of uncompaction. The intracytoplasmic uncompacted space is contiguous with the mesaxon, which may also be enlarged (Vital et al. 1983). Loss of compaction can involve part or all of the myelin sheath thickness. Because uncompacted myelin often shows an intimate relation with Schmidt–Lanterman clefts, apparent changes must be interpreted with caution. Some of the pictures used to illustrate "uncompacted myelin" seem to us to represent minimally

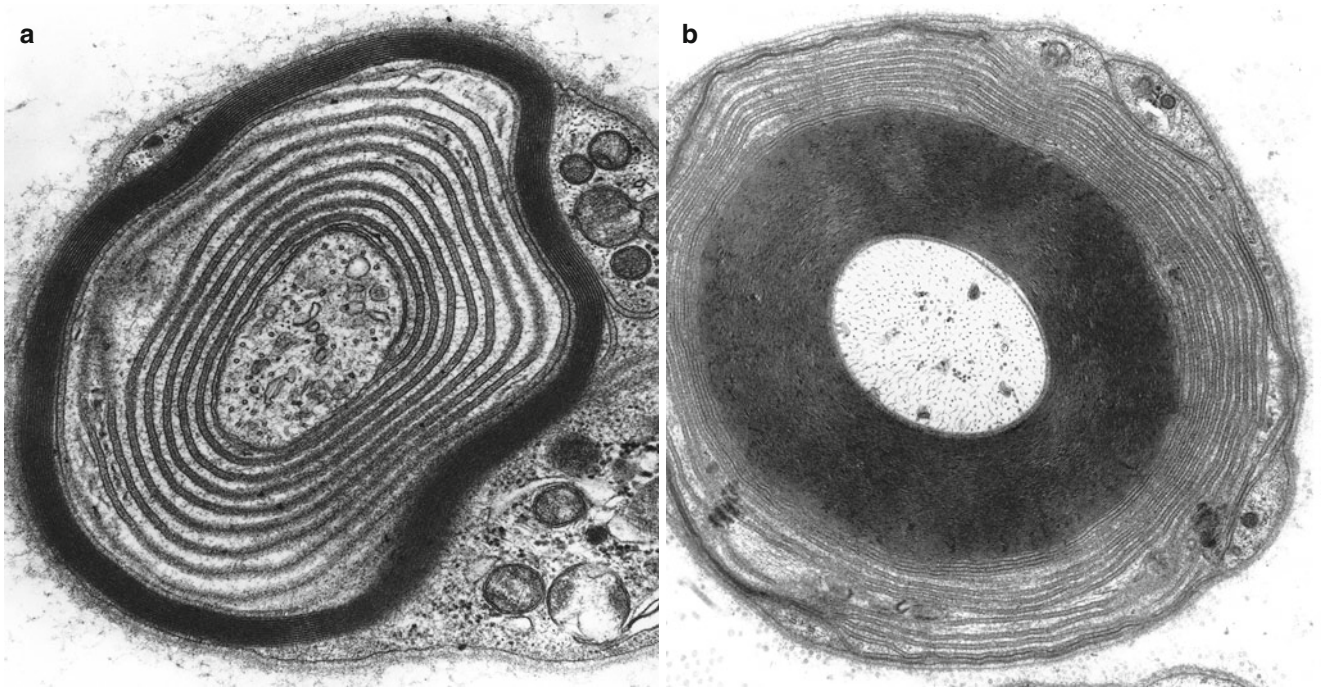

Fig. 5.13 Uncompacted myelin. The innermost (**a**) and outermost (**b**) layers of Schwann cell cytoplasm are uncompacted – POEMS (**a** 12,000×; **b** 10,000×)

Table 5.1 Neuropathies with uncompacted myelin

Human disease	
POEMS syndrome	Vital et al. (1994)
IgG or IgA paraprotein-associated neuropathy not meeting criteria for POEMS	Vital et al. (1983)
Hereditary neuropathy with liability to pressure palsies	Yoshikawa and Dyck (1991)
GBS	Brechenmacher et al. (1987)
CIDP	Vital et al. (1990), Fig. 18
Acute demyelinating neuritis with portosystemic shunt	Vital et al. (1978)
Paraneoplastic	Lamarche and Vital (1987)
Congenital dysmyelinating neuropathy	Asbury and Johnson (1978), p. 135; Lyon (1969)
Vincristine neuropathy	Vital and Vallat (1987), Fig. 89
Experimental data	
Experimental allergic neuritis	King and Thomas (1984)
Irradiation	Masurovsky et al. (1967)
Trembler mouse	Ayers and Anderson (1975)

altered Schmidt–Lanterman clefts of little significance (reference Vital et al. 1994 Fig. 4 vs. our material).

Most reports of uncompacted myelin in humans have occurred in the setting of the POEMS syndrome, where UCM was said to occur in 1–16 % of internodal cross sections (Vital et al. 1994). Ohnishi and Hirano (1981), who first described this alteration, noted that UCM often appeared to arise from abnormal terminal myelin loops, with an appearance similar to that illustrated by Allt (1969) while studying remyelination. Indeed, some authors have suggested that UCM results from disruption of remyelination, not as a primary change of compact myelin (Vital et al. 1983). Immunoglobulin deposits have not been detected on the involved membrane (Vital et al. 1994). Yoshikawa and Dyck (1991) studied uncompacted myelin in hereditary neuropathy with liability to pressure palsies (HNPP) and suggested an abnormality of a myelin protein involved in lack of compaction. P_0 protein, thought to be important for compaction of both the major dense line and the intraperiod line, was considered a good candidate, and experiments involving disruption of the myelin P_0 protein have resulted in production of some uncompacted myelin (Giese et al. 1992). The Trembler mouse, in which uncompacted myelin is a prominent ultrastructural feature (Ayers and Anderson 1975; Low 1976), has a point mutation in the PMP-22 gene (Suter et al. 1992). This mutation seems worthy of note given that deletion of a part of chromosome 17 which

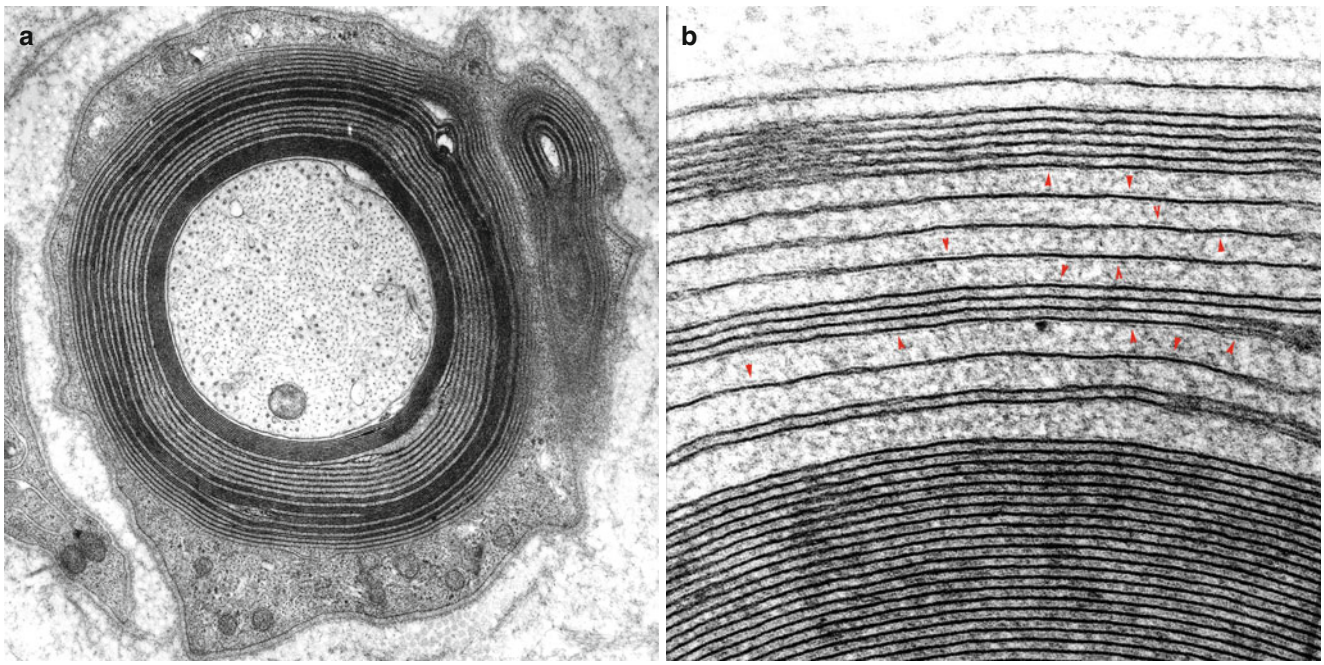

Fig. 5.14 Widely spaced myelin. (**a**) Typical appearance in a patient with circulating IgM paraprotein and demyelinating neuropathy. (**b**) WSM is caused by separation of the intraperiod line (*arrowheads*) (**a** 25,000×; **b** 137,000×)

Table 5.2 Neuropathies with widely spaced myelin

Human disease	
Paraproteinemic neuropathy, IgM≫IgG or IgA	
CIDP	King and Thomas (1984), Vital et al. (1986)
GBS	Vallat et al. (1994)
Experimental material	
Soaking in hypotonic solution prior to fixation	King and Thomas (1984)
Experimental allergic neuritis	King and Thomas (1984), Lampert et al. (1977)
Injection of GBS or EAN serum into peripheral nerve or nerve culture	Hirano et al. (1971), Raine and Bornstein (1979)
Irradiation	Masurovsky et al. (1967)
Silver nitrate-induced cerebral edema	Hirano et al. (1965)

includes the PMP-22 gene that occurs in HNPP results in a human disease where uncompacted myelin may be seen (Yoshikawa and Dyck 1991).

Widely Spaced Myelin

Widely spaced myelin (WSM) results from the separation of the intraperiod line (IPL), which normally comprises two thin lines 2–4 nm apart; in WSM this distance increases to 20–30 nm, causing the normal major dense lines to be separated by a space contiguous with the extracellular compartment (Fig. 5.14a, b). The striking regularity of this increased myelin periodicity distinguishes it from artifacts and from nonspecific degenerative changes. Widely spaced myelin is most often seen in the outermost myelin lamellae. Alternatively, WSM may remain confined to inner layers or occur throughout the entire thickness of the sheath. The abnormality may begin at the external mesaxon and continue into the myelin lamellae, and the external mesaxon itself may be dilated or misshapen. A moderately electron-dense granular material is often present in the widened extracellular space. Anywhere from a few fibers to every visible myelinated axon may show WSM in a biopsy specimen, and small myelinated axons often seem prominently involved (Pollard et al. 1985). An increased separation can also be seen between layers of the Schmidt–Lanterman cleft, between adjacent terminal myelin loops at the paranodal area, and between the Schwann cell and its basement membrane, all areas corresponding to the extracellular space (Jacobs and Scadding 1990). The normal adaxonal gap, normally 13 nm with narrowing to 4 nm at junctional sites, may be increased in width with apparent disruption of the junctions (King and Thomas 1984).

The vast majority of cases displaying WSM in humans have been associated with a circulating paraprotein, usually (but not invariably) with activity against myelin-associated

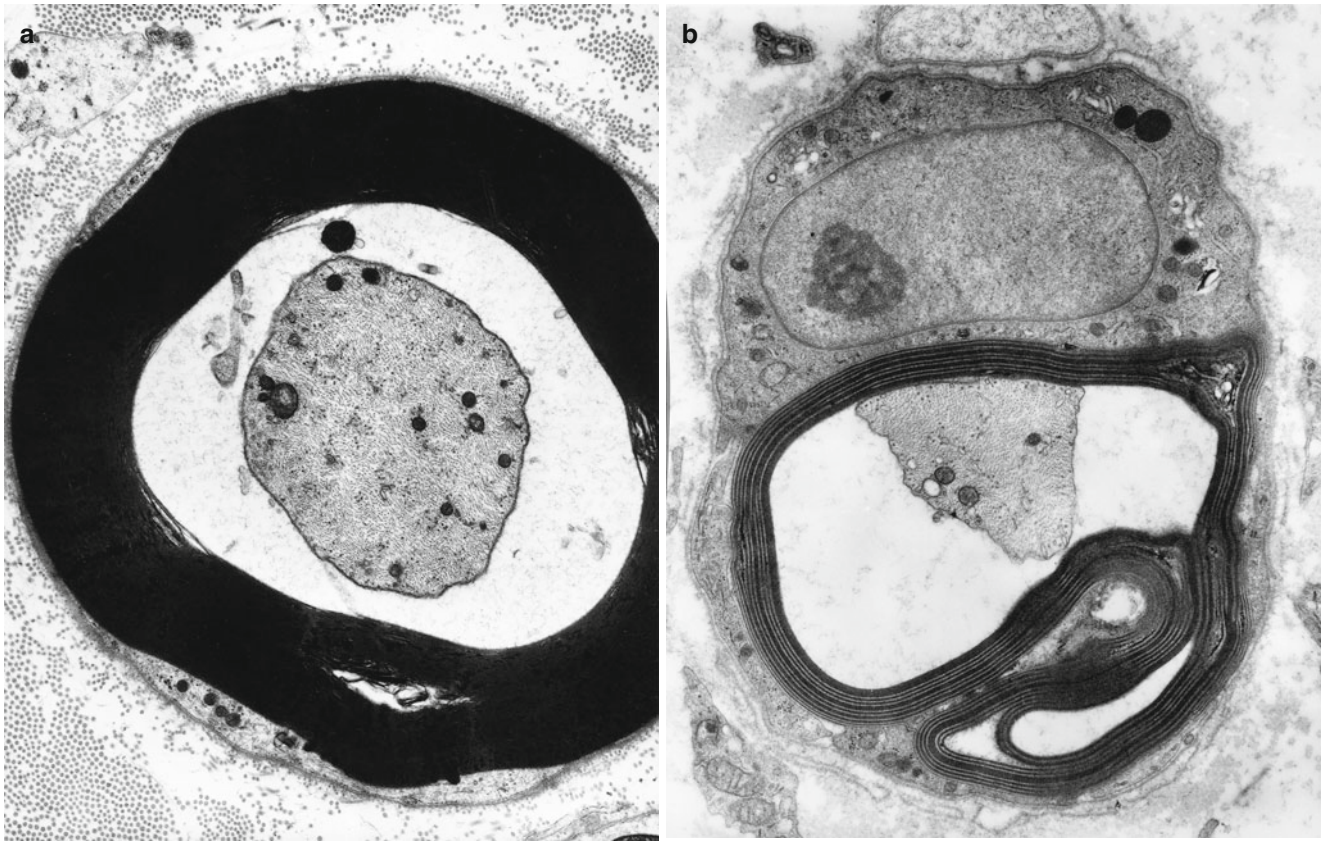

Fig. 5.15 Intramyelinic edema is seen in uremic neuropathy (**a**) and IgM paraprotein (**b**) (**a** 8,000×; **b** 12,780×)

glycoprotein (MAG) (Table 5.2). Indeed the association with IgM paraprotein is so strong that one wonders if the rare cases of WSM occurring outside this setting were also due to an occult IgM paraprotein or polyclonal immunoglobulin with anti-MAG or other myelin antigen activity. Myelin-associated glycoprotein is an outer cell surface antigen thought to be operative in cell adhesion and separation. Perhaps interference with this function results in the separation of myelin (Attia et al. 1989). The paraprotein has been conclusively immunolocalized to the extracellular space within the widely spaced myelin (Lach et al. 1993), adding weight to this hypothesis. In a model of experimental allergic encephalitis, it was possible to demonstrate unequivocally that widely separated myelin lamellae were associated with deposition of immunoglobulin at the outer aspect of both half-membrane leaflets making up the intraperiod line (Johnson et al. 1979). Immunoglobulins are positively charged molecules that will be strongly attracted to the negatively charged membranes lining the extracellular space within the intraperiod line. Separation of the myelin lamellae may result from interference with the electrostatic forces that maintain normal compaction (Ropte et al. 1990; Thomas et al. 1993).

King and Thomas (1984) produced WSM simply by soaking the nerve in hypotonic solution prior to fixation, indicating that abnormal hydration of the myelin sheath can cause this change. Other authors who were able to produce WSM without immune manipulations, for example, radiation (Masurovsky et al. 1967) or silver nitrate impregnation (Hirano et al. 1965), also postulated the occurrence of "intramyelinic edema."

"Loosened myelin" is a different myelin alteration that has been illustrated in the literature and which should not be mistaken for WSM. In loosened myelin the myelin lamellae are irregularly separated and wavy. This condition has been detected in leprous neuropathy and metachromatic leukodystrophy, but also can be seen in other neuropathies. We share the opinion of Vital and Vallat that loosened myelin may be artifactual (Vital and Vallat 1987, p 71).

Intramyelinic Edema

Although at first glance myelinated axons in which axons are smaller than expected for the overall MF size were thought to represent atrophic axons, the current explanations of this ultrastructural appearance is that it represents intramyelinic edema involving the periaxonal lamellae (Fig. 5.15a, b).

Table 5.3 Demyelinating neuropathies with Schwann cell inclusions

Storage diseases (Chap. 20)
Metachromatic leukodystrophy
Krabbe leukodystrophy
Niemann–Pick disease
Farber disease
Adrenoleukodystrophy
Cerebrotendinous xanthomatosis
Amiodarone, perhexiline, chloroquine
Leprosy (Chap. 12)
CMV neuritis

5.2.3 Schwannopathy

Many of the demyelinating neuropathies can be thought of as "schwannopathies," where the Schwann cell metabolic machinery is unable to maintain the myelin sheath. Schwann cell inclusions may be a critical clue to this situation (Table 5.3). Nonspecific evidence of a "sick" or "stressed" Schwann cell may be seen, such as a proliferation, or conversely a loss, of endoplasmic reticulum, vacuolation, accumulation of glycogen, dysmorphic mitochondria, accumulations of electron-dense amorphous or lamellated inclusions, and watery distention of the normally thin mesaxons and rims of Schwann cell cytoplasm surrounding the myelin sheath.

5.2.3.1 Alterations in Myelin Sheath Thickness and Form

"Tomaculous" alterations refer to fibers with a myelin sheath which is thickened circumferentially or eccentrically and may show prominent focal outfoldings and infoldings. This abnormality is discussed elsewhere and most often is associated with HNPP. Conversely, hypomyelinating neuropathy shows a diffuse picture of myelin sheaths too thin for axonal diameter. Diffuse hypomyelination may be congenital or may result from widespread demyelination and remyelination. Rare congenital neuropathies have been reported with "unstable" myelin showing a striking tendency to fragment and form globular debris in association with demyelination.

5.2.4 Secondary Demyelination

More than a century ago, Gombault (1886) considered that demyelination can occur as a consequence of axonal disease. In the 1970s, Dyck and colleagues (1984b) studied a number of clinical and experimental models of peripheral nerve disease and demonstrated convincingly that the myelin changes seen are actually caused by axonal abnormalities. Prior to the clear delineation of this concept, some neuropathies now recognized as primarily axonal had been misinterpreted as predominantly demyelinating, including diabetes, porphyria, and uremia.

5.2.4.1 Experimental Data Supporting Secondary Demyelination

Dyck and colleagues (1971) conducted the first quantitative study of secondary demyelination in uremic neuropathy when they examined biopsied sural nerve fascicles from ankle and midcalf levels in two patients with renal failure and neuropathy. These biopsies provided unequivocal evidence of demyelination, but this occurred in a nonrandom fashion along certain axons. In more proximal nerve segments, the most common abnormality was myelin wrinkling, whereas the distal nerve segment demonstrated predominantly axonal degeneration and segmental demyelination. Individual teased fibers showing segmental myelin change were then cut in sequential cross section along their length; the axons found within were extremely atrophic. Such data, and similar results in Friedreich's ataxia nerves (Dyck and Lais 1973), suggested that in these situations a distal axonal atrophy resulted in segmental demyelination. Although convincing, the possibility that the Schwann cell was still somehow defective in both uremia and Friedreich's ataxia could not be entirely dismissed. Dyck and colleagues provided conclusive evidence for secondary demyelination in their permanent axotomy model, taking advantage of the fact that after nerve transection the proximal segment becomes somewhat atrophic (Dyck et al. 1981). With time, myelin wrinkling evolved into frank demyelination without significant axonal loss proximal to the site of axotomy. In the current conception of secondary demyelination, axonal atrophy results in myelin wrinkling, followed by paranodal or segmental demyelination, then remyelination. Why the myelin wrinkles when the axon atrophies remains unclear. Is it a simple mechanical problem, with loss of support to the inner myelin layers or even traction on them (Dyck et al. 1984b)? Or is there an interruption of crucial physiologic interactions between the axon and Schwann cell?

5.2.4.2 Pathological Alterations in Secondary Demyelination

Distinguishing secondary demyelination from primary demyelination can prove difficult. In practice, one simply weighs the balance of axonal disease vs. that of myelin change. Occasional thinly myelinated fibers are likely to be a secondary alteration if axonal dropout or active degeneration is very prominent. With abundant evidence of active or chronic demyelination in the presence of minimal axonal dropout and active degeneration, one suspects that the demyelination is primary. The difficulty arises when significant amounts of both axonal and myelin alterations are present, a common situation in practice.

Some observations may provide helpful clues. Onion bulbs and naked axons can occur in secondary demyelination, but in general should lead one to favor a primary demyelinating process. If some of the specific alterations of

primary demyelination discussed above are seen (Schwann cell inclusions, macrophage-mediated myelin stripping, widely spaced myelin, etc.), then one would reasonably diagnose a primary disease of myelin or Schwann cells. Electron microscopic examination can prove very helpful in deciding whether demyelination is occurring around normal axons or around axons which show signs of pathology, such as atrophy, accumulations of organelles, or even disintegration. Light microscopy and nerve teasing do not provide this information.

After weighing these various factors, it is usually possible to decide whether the process is likely a primary demyelination or a primary axonopathy. In those cases where the distinction is still not possible, more involved teased fiber and quantitative techniques are very helpful. A fiber size histogram demonstrating a bimodal peak with a shift towards to the left is suggestive of the presence of axonal attenuation (Ohi et al. 1985). Demonstration that the myelin internode length is inappropriately long for the axon diameter allows a similar inference (Ohi et al. 1985). However, the most conclusive way of making the distinction involves the use of teased fiber preparations. In secondary demyelination, "sick" axons with many abnormal internodes along their length are intermingled with healthy axons which have a full complement of normal internodes. Thus, there is a clustering of abnormal myelin segments along certain axons (Dyck and Lais 1973). In primary demyelination the abnormal segments are spread randomly through the fibers, as some experimental lead neuropathy models demonstrate (Windebank and Dyck 1984).

While teased nerve preparations are necessary in research situations, we almost never make use of them in practice. For satisfactory teasing studies, at least 100 fibers with 5 intact internodes must be obtained to derive statistically useful data (Dyck et al. 1971). Routinely performing such analysis is beyond the reach of most pathology laboratories, including our own. Either there is a lack of expert technologists who can carry this meticulous task or the procedure proves too expensive and time consuming. We do not believe that the information gained is enough to justify the cost of maintaining the ability to provide this service. Deciding whether the demyelination is secondary or primary may help in narrowing the differential diagnosis, but never gives a final etiologic diagnosis. In those instances where an etiologic diagnosis is possible, it is almost always reached by identification of specific changes in the nerve interstitium using cross-sectional views. Moreover, the appearance of myelin and axons is very well visualized on appropriately stained plastic-embedded material.

Some authors do not try to make the distinction between primary or secondary demyelination or call the demyelination "primary" if myelin loss exceeds axon loss (Honavar et al. 1991). Another approach involves labeling as "predominantly axonal" those biopsies where axonal changes are more prominent than demyelinating changes and as "predominantly demyelinating" those biopsies where myelin alterations are more prominent. Intermediate features are labeled as either mixed or indeterminate (Barohn et al. 1989; Logigian et al. 1994). We recognize that these approaches are subjective and prone to error in inexperienced hands, but nevertheless feel that they are a necessary concession to pragmatism and adequate for routine clinical work.

5.2.4.3 The Clinical Significance of Secondary Demyelination

Conditions in which secondary demyelination has been conclusively shown to be important include uremia (Dyck et al. 1971), Friedreich's ataxia (Dyck and Lais 1973), some paraproteinemic neuropathies (Ohi et al. 1985), and thiamine deficiency (Ohnishi et al. 1980). Conditions in which secondary demyelination is likely to be important include some paraneoplastic neuropathies (Schlaepfer 1974), hexacarbon toxicity (Chap. 18), and Tangier disease (Pollock et al. 1983). However, there is probably some secondary demyelination in any axonal process including amyloidosis (Said et al. 1984), vasculitis (Nukada and Dyck 1987), and all distal axonopathies. Interestingly, an abundance of experimental data suggests that CMT-1 is also a distal axonopathy with secondary demyelination, yet alterations in peripheral myelin protein (PMP-22) are believed to somehow cause the disease in most patients. Clearly, the complexities of axon–Schwann cell interactions make determining which one is primarily responsible for a neuropathy a difficult task when done purely on morphologic grounds.

5.2.5 Mechanisms of Demyelination

A few of the mechanisms by which demyelination can occur have been discussed previously including macrophage- and antibody-mediated attack, demyelination secondary to axonal atrophy, and the role of calcium influx with activation of phospholipases (Smith and Hall 1988) or endogenous proteases (Koski 1992; Banik 1992). Such calcium influx might result from activation of the complement membrane attack complex (Koski 1992). Myelinotoxic products of the inflammatory response may be important in granulomatous and inflammatory neuropathies. Macrophage-derived neutral proteases can produce selective demyelination in vitro (Said and Hontebeyrie-Joskowicz 1992; Cammer et al. 1978). In diphtheria, historically a cornerstone of the study of demyelinating neuropathies, the toxin does not "attack" the myelin, but rather inhibits Schwann cell protein synthesis (Pappenheimer and McGill 1973) interfering with the normal turnover of myelin P_0 and basic proteins (Pleasure et al. 1973). Similarly, lead neuropathy is probably caused by an impairment of Schwann cell metabolism, but the molecular mechanisms are unclear (Windebank and Dyck 1984).

5.3 Remyelination

5.3.1 Normal Remyelination

The experimental models from which the discussion below is derived are based on a variety of demyelinating mechanisms, including recurrent immunization with myelin (Pollard et al. 1975), injection with lysophosphatidylcholine (Hall 1983), exposure to diphtheria toxin (Allt 1969), intoxication with iminodipropionitrile (Griffin et al. 1987), and mechanical pressure (Dyck 1969). The process of remyelination appears to be independent of the mechanism of demyelination. Whether originally macrophage mediated or not, debris from demyelinating fibers is removed by macrophages, attracted to the site by as yet unclear signals (Griffin et al. 1993).

In experimental animals, the process of regeneration of the myelin sheath begins as soon as 2 days after demyelination, with a proliferation of SCs (Griffin et al. 1987). Schwann cells that have lost their myelin sheath, and perhaps neighboring nonmyelinating Schwann cells, provide the pool of proliferating cells (Griffin et al. 1990). At the onset of remyelination, several SCs may be visible within the basal lamina of one axon (Ballin and Thomas 1969b; Pollard et al. 1975; Dyck 1969). Only one Schwann cell, however, succeeds in capturing and myelinating the axon, while the others are displaced peripherally, undergo involutional changes, and diminish in number with time (Fig. 5.17). Necrosis of these supernumerary Schwann cells can be observed (Pollard et al. 1975). One characteristic of an axon that has become demyelinated and remyelinated is the presence of folds of redundant basement membrane, probably left behind by the now-obsolescent SCs that were produced in the early stages of the remyelinating process (Fig. 5.16a) (Dyck 1969).

Remyelinating SCs often have an abundance of RER, mitochondria, Golgi membranes, and free ribosomes and are rich in cytoplasm (Fig. 5.17). As successive turns of myelin are laid down, the most superficial lamellae are the first to reach that part of the axon destined to form the new node of Ranvier (Prineas 1972). Initially the myelin lamellae are poorly compacted but this resolves as successive turns are laid down (Fig. 5.16b). By four weeks after the demyelinating event, axons have a thin new compact myelin sheath which continues to grow for several months thereafter and eventually reaches a thickness which does not quite equal that of the original (Pollard et al. 1975).

The mechanism of remyelination depends to a certain extent on the size of the demyelinated segment. If only a small paranodal segment of myelin is lost, it may be replaced by a single, new, "intercalated" internode (Allt 1969; Griffin et al. 1987). Where the paranodal demyelinated segment is very short (<15 μm), an extension of the already present but retracted Schwann cell cytoplasm might recover the denuded

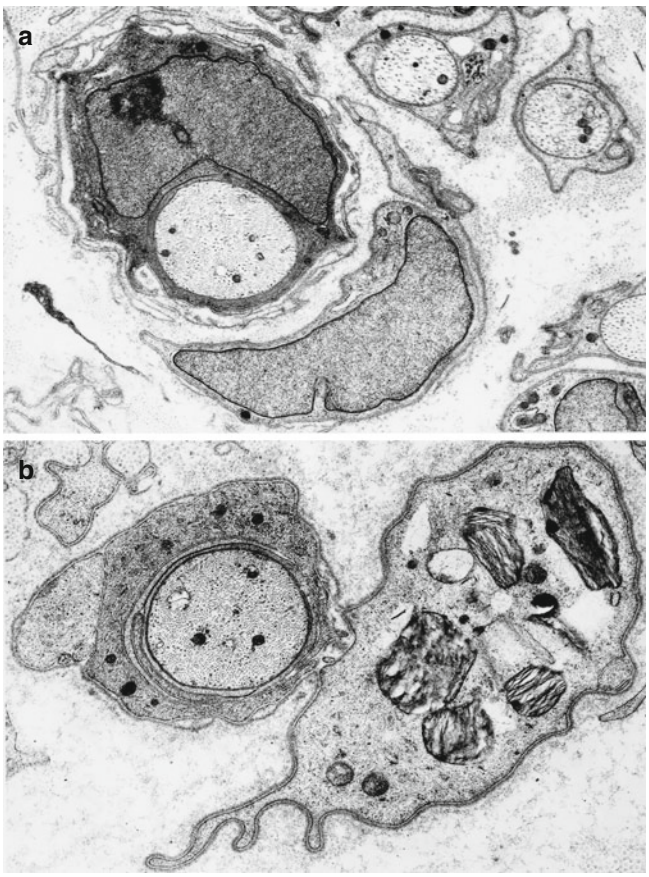

Fig. 5.16 Remyelination. Remyelinating fibers show 2–3 spirals of uncompacted Schwann cell cytoplasm. Redundant basal lamina and a displaced denervated Schwann cell ("S") are shown in (**a**). In (**b**) a displaced Schwann cell process containing pi granules is invested by basal lamina which is continuous with that of the remyelinating fiber (**a** 13,680×; **b** 16,416×)

Fig. 5.17 Remyelinating fiber with thin compacted myelin sheath. The Schwann cell displays prominent Golgi complex (*arrows*), abundant RER, and a redundant basal lamina (18,616×)

axon segment, without formation of a new internode (Allt 1969). If a whole internode is demyelinated, it is typically repaired through the formation of several much smaller internodes. This process results in an increased variability of internodal length, as short intercalated nodes intermingle with longer normal undisturbed internodes.

Nearly all detailed descriptions of remyelination have commented on the association of unmyelinated axons with the supernumerary Schwann cells around a remyelinating axon (Pollard et al. 1975; Dyck 1969; Hall 1983). Such unmyelinated fibers probably correspond to those routinely incorporated into the Schwann cell layers of onion-bulb formations. The origin of these axons is unclear. They may be seen even when there is no evidence of axonal degeneration (Hall 1983). It is possible that these unmyelinated axons are collateral sprouts emerging from a demyelinated but intact axon. The observation that such unmyelinated axonal sprouts decrease in number with time favors this hypothesis, since this finding would not be expected if these profiles represented stable, previously existing, unmyelinated fibers (Pollard et al. 1975). This hypothesis receives further support from the observation that these unmyelinated axons can sometimes be found within the original basal lamina (Pollard et al. 1975). However, the work of Griffin and colleagues (1987) indicates that nonmyelinating Schwann cells nearby a demyelinated axon can become involved in the process of remyelination, suggesting that this involvement may be the origin of some unmyelinated axons associated with remyelinating fibers.

Remyelination may occur aberrantly as shown (Fig. 5.18) in which a central unmyelinated axon and its surrounding Schwann cell are themselves surrounded by a myelin sheath. In some conditions, uninjured Schwann cells nearby demyelinated or degenerating axons can be stimulated to proliferate, which may underlie a very rare mitosis (Fig. 5.19) in an otherwise normal appearing Remak bundle.

Fig. 5.18 Aberrant remyelination. A myelinated sheath surrounds a Schwann cell nucleus adjacent to an unmyelinated axon which is partially surrounded by a few turns of uncompacted Schwann cell membrane (12,000×)

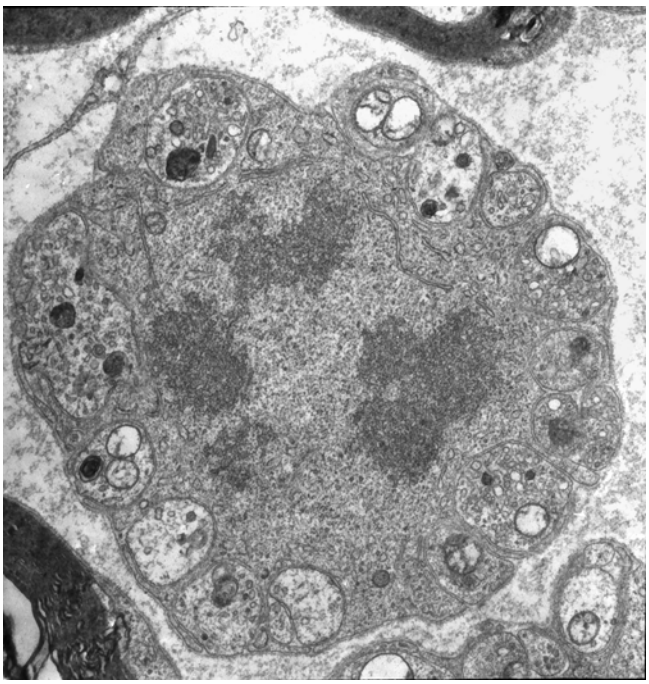

Fig. 5.19 Demonstration of a mitotic figure in an otherwise normal Schwann cell composing a Remak bundle is a very rare occurrence (12,000×)

5.3.2 Onion-Bulb Formation

Animal models have demonstrated that a single demyelinating/remyelinating event is insufficient to create onion bulbs, but recurrent or continuing demyelinating insults can produce onion bulbs in great numbers (Pollard et al. 1975; Dyck 1969). However, if after one complete cycle of demyelination and remyelination the myelinated axon completely returns to normal (except for a slightly thinner myelin sheath), it is unclear how recurrent events produce the onion bulb. Certainly in some models of recurrent demyelination, it has been quite difficult to create these formations (Raine 1977; Hall 1983).

Ultrastructural observations suggest that with each cycle of demyelination, Schwann cell processes that do not succeed

in capturing an axon become atrophic and are displaced centrifugally by the new Schwann cell that remyelinates the axon. Ordinarily these supernumerary cells become obsolete so that only one Schwann cell is associated with the axon. One explanation for onion-bulb formation would be that if demyelination occurs again before the orderly process of elimination of supernumerary Schwann cells is complete, excessive numbers of surviving Schwann cells remain around the axon and create the onion bulb (Pollard et al. 1975). Repetitive cycles build up the concentric array of flattened Schwann cell processes and their basement membranes that makes up an onion bulb. Diseases in which demyelination is occurring concurrently with remyelination for prolonged periods should produce the most dramatic onion bulbs, for example, the inherited hypertrophic neuropathies or CIDP. Authors who have had difficulty producing "true" onion bulbs despite exposing the nerve to recurrent episodes of demyelination have suggested that other factors in addition to recurrent demyelination/remyelination are required to produce onion bulbs, for example, hereditary or acquired metabolic defects of the Schwann cell (Hall 1983; Raine 1977).

Observations in human disease (Pleasure and Towfighi 1972) and experimental models (Pollard et al. 1975) suggest that the presence of onion bulbs indicates a demyelinating process that has been active for at least several months, and the longer the duration of the demyelinating process, the more onion bulbs are seen. Although onion bulbs are far more likely to be seen in diseases causing primary demyelination, demyelination secondary to axonal disease may also cause onion-bulb formation. This occurrence presumably depends on the chronicity of the process and on how many times the axon sheds and rebuilds its myelin sheath before finally dying (Griffin and Price 1981).

References

Aguayo AJ, Epps J, Charron L, Bray GM (1976) Multipotentiality of Schwann cells in cross-anastomosed and grafted myelinated and unmyelinated nerves. Brain Res 104:1–20

Allt G (1969) Repair of segmental demyelination in peripheral nerves. Brain 92:639–646

Allt G (1983) The node of Ranvier in experimental allergic neuritis. An electron microscopic study. J Neurocytol 4:63–76

Arnason BGW, Soliven B (1993) Acute inflammatory demyelinating polyneuropathy. In: Dyck PJ, Thomas PK et al (eds) Peripheral neuropathy, 3rd edn. W.B. Saunders, Philadelphia, pp 1437–1497

Asbury AKB, Arnason G, Adams RD (1969) The inflammatory lesion in idiopathic polyneuritis. Medicine 48:173–215

Asbury AK, Johnson PC (1978) Pathology of peripheral nerve, vol 9, Major problems in pathology. WB Saunders, Philadelphia

Aszodi A, Legate KR, Nakchbandi I et al (2006) What mouse mutants teach us about extracellular matrix function. Annu Rev Cell Dev Biol 22:591–621

Attia J, Tropak M, Johnson PW et al (1989) Modulated adhesion: a proposal for the role of myelin-associated glycoprotein in myelin wrapping. Clin Chem 35:717–720

Ayers MM, Anderson R (1975) Development of onion bulb neuropathy in the Trembler mouse. Acta Neuropathol 32:43–59

Babel J, Bischoff A, Spoendlin H (1970) Ultrastructure of the peripheral nervous system and sense organs. CV Mosby, St. Louis, p 48

Ballin RH, Thomas PK (1969a) Changes at the nodes of Ranvier during wallerian degeneration: an electron microscope study. Acta Neuropathol 14:237–249

Ballin RH, Thomas PK (1969b) Electron microscope observations on demyelination and remyelination in experimental allergic neuritis. 2 Remyelination. J Neurol Sci 8:225–237

Banik NL (1992) Pathogenesis of myelin breakdown in demyelinating diseases: role of proteolytic enzymes. Crit Rev Neurobiol 6:257–271

Barohn RJ, Kissel JT, Warmolts JR et al (1989) Chronic inflammatory polyradiculoneuropathy. Clinical characteristics, course, and recommendations for diagnostic criteria. Arch Neurol 46:878–884

Behse F (1990) Morphometric studies on the human sural nerve. Acta Neurol Scand Suppl 132:1–38

Ben Jelloun-Dellagi S, Dellagi K, Burger D et al (1992) Childhood neuropathy with autoantibodies to myelin glycoprotein P0. Ann Neurol 32:700–702

Berthold CH, Rydmark M (1983) Electron microscopic serial section analysis of nodes of Ranvier in lumbosacral spinal roots of the cat: ultrastructural organization of nodal compartments in fibres of different sizes. J Neurocytol 12:475–505

Birchem R, Mithen FA, L'Empereur KM et al (1987) Ultrastructural effects of Guillaine-Barre serum in cultures containing only rat Schwann cells and dorsal root ganglion neurons. Brain Res 421:173–185

Birchmeier C, Nave K-A (2008) Neuregulin-1, a key axonal signal that drives Schwann cell growth and differentiation. Glia 56:1491–1497

Bleasel AF, Hawke SH, Pollard JD et al (1993) IgG monoclonal paraproteinemia and peripheral neuropathy. J Neurol Neurosurg Psychiatry 56:52–57

Brechenmacher C, Vital C, Deminiere C et al (1987) Guillaine-Barre syndrome: an ultrastructural study of peripheral nerve in 65 patients. Clin Neuropathol 6:19–24

Brown MJ, Rosen JL, Lisak RP (1987) Demyelination in vivo by Guillaine-Barre syndrome and other human serum. Muscle Nerve 10:263–271

Buchthal F, Carlsen F, Behse F (1987) Schmidt-Lanterman clefts: a morphometric study in human sural nerve. Am J Anat 180:156–160

Bunge MB (1993) Schwann cell regulation of extracellular matrix biosynthesis and assembly. In: Dyck PJ, Thomas PK et al (eds) Peripheral neuropathy, 3rd edn. WB Saunders, Philadelphia, pp 299–316

Buttermore ED, Thaxton CL, Bhat MA (2013) Organization and maintenance of molecular domains in myelinated axons. J Neurosci Res 91:603–622

Cammer W, Blood BR, Norton WT et al (1978) Degradation of basic protein in myelin by neutral proteases secreted by stimulated macrophages: a possible mechanism of inflammatory demyelination. Proc Natl Acad Sci U S A 75:1554–1558

Carlsen F, Knappeis GG, Behse F (1974) Schwann cell length in unmyelinated fibres of human sural nerve. J Anat 117:463–467

Carpenter S (1972) An ultrastructural study of an acute fatal case of the Guillain-Barre Syndrome. J Neurol Sci 15:125–140

Celio MR (1976) Die Schmidt-Lantermann'schen Einkerburgen der Myelinscheide des Mauthner-axons: Orte Longitudinalen Myelinwachstums. Brain Res 108:221–235

Chernousov MA, Yu W-M, Chen Z-L (2008) Regulation of Schwann cell function by the extracellular matrix. Glia 56:1498–1507

Cornblath DR, McArthur JC, Kennedy PGE et al (1987) Inflammatory demyelinating peripheral neuropathies associated with human T-cell lymphotropic virus type III infection. Ann Neurol 21:32–40

Dal Canto M, Wisniewski HM, Johnson AB et al (1975) Vesicular disruption of myelin in autoimmune demyelination. J Neurol Sci 24:313–319
Dyck PJ (1969) Experimental hypertrophic neuropathy. Arch Neurol 21:73–95
Dyck PJ, Lais AC (1973) Evidence for segmental demyelination secondary to axonal degeneration in Friedreich's ataxia. In: Kakulas BK (ed) Clinical studies in myology. Excerpta Medica, Amsterdam, pp 253–263
Dyck PJ, Lambert EH (1970) Polyneuropathy associated with hypothyroidism. J Neuropathol Exp Neurol 29:631–658
Dyck PJ, Johnson WJ, Lambert EH, O'Brien PC (1971) Segmental demyelination secondary to axonal degeneration in uremic neuropathy. Mayo Clin Proc 46:400–431
Dyck PJ, Lais AC, Karnes JL et al (1981) Permanent axotomy, a model of axonal atrophy and secondary segmental demyelination and remyelination. Ann Neurol 9:575–583
Dyck PJ, Karnes J, Lais A et al (1984a) Pathologic alterations of the peripheral nervous system of humans. In: Dyck PJ, Thomas PK et al (eds) Peripheral neuropathy, 2nd edn. WB Saunders, Philadelphia, pp 760–870
Dyck PJ, Nukada H, Lais AC, Karnes JL (1984b) Permanent axotomy: a model of chronic neuronal degeneration preceded by axonal atrophy, myelin remodeling, and degeneration. In: Dyck PJ, Thomas PK et al (eds) Peripheral neuropathy, 2nd edn. W.B. Saunders, Philadelphia, pp 666–690
Dyck PJ, Giannini C, Lais A (1993) Pathologic alterations of nerves. In: Dyck PJ, Thomas PK et al (eds) Peripheral neuropathy, 3rd edn. WB Saunders, Philadelphia, pp 30–34, Table 30–4
Eames RA, Gamble HJ (1970) Schwann cell relationships in normal human cutaneous nerves. J Anat 106:417–435
Epstein LG, Prineas JW, Raine CS (1983) Attachment of myelin to coated pits on macrophages in experimental allergic encephalomyelitis. J Neurol Sci 61:341–348
Evans MJ, Finean JB, Woolf AL (1965) Ultrastructural studies of human cutaneous nerve with special reference to lamellated cell inclusions and vacuole containing cells. J Clin Pathol 18:188–192
Fardeau M, Engel KW (1969) Ultrastructural study of a peripheral nerve biopsy in Refsum's disease. J Neuropathol Exp Neurol 28:278–294
Filbin MT, Tennekoon G (1991) The role of complex carbohydrates in adhesion of the myelin protein P0. Neuron 7:845–855
Friede RL, Beuche W (1985) A new approach toward analysing peripheral nerve fiber population. I. variance in sheath thickness corresponds to different geometric proportions of the internodes. J Neuropathol Exp Neurol 44:60–72
Friede RL, Bischhausen R (1982) How are sheath dimensions affected by axon caliber and internodal length? Brain Res 235:335–350
Friede RL, Bruch W (1993) Macrophage functional properties during myelin degradation. Adv Neurol 59:327–336
Friede RL, Meier T, Diem M (1981) How is the exact length of an internode determined? J Neurol Sci 50:217–228
Ghabriel MN, Allt G (1979) The role of Schmidt-Lanterman incisures in Wallerian degeneration. I. A quantitative teased fiber study. Acta Neuropathol 48:83–93
Ghabriel MN, Allt G (1981) Incisures of Schmidt-Lanterman. Prog Neurobiol 17:25–58
Gibbels E (1989) Morphometry of unmyelinated nerve fibers. Clin Neuropathol 8:179–187
Giese KP, Martini R, Lemke G et al (1992) Mouse P0 gene disruption leads to hypomyelination, abnormal expression of recognition molecules, and degeneration of myelin and axons. Cell 71:565–576
Goebel HH, Zeman W, Pilz H (1976) Ultrastructural investigations of peripheral nerves in Neuronal Ceroid -Lipofuscinoses (NCL). J Neurol 213:295–303
Gombault M (1886) Sur les lesion de la nevrite alcoolique. C R Acad Sci Hebd Seances Acad Sci D 102:439–440
Griffin JW, Price DL (1981) Demyelination in experimental IDPN and hexacarbon neuropathies: evidence for an axonal influence. Lab Invest 45:130–141
Griffin JW, Thompson WJ (2008) Biology and pathology of nonmyelinating Schwann cells. Glia 56:1518–1531
Griffin JW, Drucker N, Benzaquen M et al (1987) Schwann cell proliferation and migration during paranodal demyelination. J Neurosci 7:682–699
Griffin JW, Stocks EA, Fahnestock K et al (1990) Schwann cell proliferation following lysolecithin-induced demyelination. J Neurocytol 19:367–384
Griffin JW, George R, Ho T (1993) Macrophage systems in peripheral nerves. A review. J Neuropathol Exp Neurol 52:553–560
Gutrecht JA, Dyck PJ (1970) Quantitative teased fiber and histological studies of human sural nerve during postnatal development. J Comp Neurol 138:117–130
Hall SM, Williams PL (1970) Studies on "incisures" of Schmidt and Lanterman. J Cell Sci 6:767–791
Hall SM (1983) The response of the (myelinating) Schwann cell population to multiple episodes of demyelination. J Neurocytol 12:1–12
Hall SM (1984) The effects of multiple sequential episodes of demyelination in the sciatic nerve of the mouse. Neuropathol Appl Neurobiol 10:461–478
Hays AP, Lee SS, Latov N (1988) Immune reactive C3d on the surface of myelin sheaths in neuropathy. J Neuroimmunol 18:231–244
Heath JW (1982) Double myelination of axons in the sympathetic nervous system. J Neurocytol 11:249–262
Hedley-White ET (1973) Myelination of rat sciatic nerve: comparison of undernutrition and cholesterol biosynthesis inhibition. J Neuropathol Exp Neurol 32:284–303
Hirano A, Zimmermann HM, Levine S (1965) The fine structure of cerebral fluid accumulation. IX. Edema following silver nitrate implantation. Am J Pathol 47:537–548
Hirano A, Cook SD, Whittaker JN et al (1971) Fine structural aspects of demyelination in vitro. The effects of Guillain-Barre serum. J Neuropathol Exp Neurol 30:249–265
Honavar M, Tharakan JKJ, Hughes RAC et al (1991) A clinicopathological study of the Guillain-Barre syndrome. Nine cases and literature review. Brain 114:1245–1269
Inouye H, Kirschner DA (1988) Membrane interactions in nerve myelin. II Determination of surface change from biochemical data. Biophys J 53:247–260
Jacobs JM (1988) On internodal length. J Anat 157:153–162
Jacobs JM, Scadding JW (1990) Morphological changes in IgM paraproteinaemic neuropathy. Acta Neuropathol 80:77–84
Johnson AB, Raine CS, Bornstein MB (1979) Experimental allergic encephalomyelitis: serum immunoglobulin binds to myelin and oligodendrocytes in cultured tissue. Ultrastructural-immunoperoxidase observations. Lab Invest 40:568–575
Kidd GJ, Ohno N, Trapp BD (2013) Chapter 5. Biology of Schwann cells. In: Said G, Krarup C (eds) Handbook clinical neurology, vol 115, 3rd series, Peripheral nerve disorders. Elsevier BV, Amsterdam, pp 55–79
King RHM, Thomas PK (1984) The occurrence and significance of myelin with unusually large periodicity. Acta Neuropathol 63:319–329
Kirshner DA, Ganser AL (1984) Diffraction studies of molecular organization and membrane interactions in myelin. In: Morell P (ed) Myelin, 2nd edn. Plenum Press, New York, chapter 2
Koski CL (1992) Humoral mechanisms in immune neuropathies. Neurol Clin 10:629–649
Lach B, Rippstein P, Atack D et al (1993) Immunoelectron microscopic localization of monoclonal IgM antibodies in gammopathy associ-

ated with peripheral demyelinative neuropathy. Acta Neuropathol 85:298–307
Lamarche J, Vital C (1987) Carcinomatous neuropathy. An ultrastructural study of 10 cases. Ann Pathol 7:98–105
Lampert PW, Garrett R (1971) Mechanism of demyelination in tellurium neuropathy. Lab Invest 25:380–388
Lampert PW, Schochet SS (1968) Demyelination and remyelination in lead neuropathy. J Neuropathol Exp Neurol 27:527–545
Lampert PW, Garrett R, Powell H (1977) Demyelination in allergic and Marek's disease virus induced neuritis. Comparative electron microscopic studies. Acta Neuropathol 40:103–110
LeBlanc AC, Poduslo JF (1990) Axonal modulation of myelin gene expression in the peripheral nerve. J Neurosci Res 26:317–326
Leibowitz S, Gregson NA, Kennedy M, Kahn SN (1983) IgM paraproteins with immunological specificity for a Schwann cell component and peripheral nerve myelin in patients with polyneuropathy. J Neurol Sci 59:153–165
Lemke G, Lamar E, Patterson J (1988) Isolation and analysis of the gene encoding peripheral myelin protein zero. Neuron 1:73–83
Linington C, Brostoff SW (1993) Peripheral nerve antigens. In: Dyck PJ, Thomas PK et al (eds) Peripheral neuropathy, 3rd edn. WB Saunders, Philadelphia, pp 404–417
Logigian EL, Kelly JJ, Adelman LS (1994) Nerve conduction and biopsy correlation in over 100 consecutive patients with suspected polyneuropathy. Muscle Nerve 17:1010–1020
Low PA (1976) Hereditary hypertrophic neuropathy in the Trembler mouse. Part II. (Histopathological studies: electron microscopy). J Neurol Sci 30:343–368
Lyon G (1969) Ultrastructural study of a nerve biopsy from a case of early infantile chronic neuropathy. Acta Neuropathol 13:131–142
Lyon G, Evrard P (1970) Sur la presence d'inclusions cristallines dans les cellules de Schwann dans divers neuropathies peripheriques. C R Acad Sci Hebd Seances Acad Sci D 271:1000–1002
Madrid R, Bradley WG, Davis CJF (1977) The peroneal muscular atrophy syndrome. Clinical, genetic, electrophysiological and nerve biopsy studies. Part 2. Observations on pathological changes in sural nerve biopsies. J Neurol Sci 32:91–122, Figure 7
Masurovsky EB, Bunge MH, Bunge RP (1967) Cytological studies of organotypic cultures of rat dorsal root ganglia following X-irradiation in vitro. II. Changes in Schwann cells, myelin sheaths, and nerve fibers. J Cell Biol 32:497–518
Mezei C (1993) Myelination in the peripheral nerve during development. In: Dyck PJ, Thomas PK et al (eds) Peripheral neuropathy, 3rd edn. W.B. Saunders, Philadelphia, pp 267–281
Michailov GV, Sereda MW, Brinkmann BG et al (2004) Axonal neuregulin-1 regulates myelin sheath thickness. Science 304:700–703
Milner P, Lovelidge CA, Taylor WA et al (1989) P0 myelin protein produces experimental allergic neuritis in Lewis rats. J Neurol Sci 790:275–285
Mirsky R, Woodhoo A, Parkinson DB et al (2008) Novel signals controlling embryonic Schwann cell development, myelination and dedifferentiation. J Peripher Nerv Syst 13:122–135
Mugnaini E, Osen KK, Schnapp B, Friedrich VL (1977) Distribution of Schwann cell cytoplasm and plasmalemmal vesicles (caveolae) in peripheral myelin sheaths. An electron microscopic study with thin sections and freeze-fracturing. J Neurocytol 6:647–668
Noback CR (1953) The protagon (Pi) granules of Reich. J Comp Neurol 99:91–100
Noback CR (1954) Metachomasia in the nervous system. J Neuropathol Exp Neurol 13:161–167
Norton WT, Cammer W (1984) Isolation and characterization of myelin. In: Morell P (ed) Myelin, 2nd edn. Plenum Press, New York, chapter 5
Nukada H, Dyck PJ (1987) Acute ischemia causes axonal stasis, swelling, attenuation, and secondary demyelination. Ann Neurol 22:311–318
Ochoa J, Mair WGP (1969) The normal sural nerve in man. I: Ultrastructure and number of fibres and cells. Acta Neuropathol 13:197–216
Ohi T, Kyle RA, Dyck PJ (1985) Axonal attenuation and secondary segmental demyelination in myeloma neuropathies. Ann Neurol 17:255–261
Ohnishi A, Tsuji S, Igisu H et al (1980) Beriberi neuropathy. Morphometric study of sural nerve. J Neurol Sci 45:177–190
Ohnishi A, Hirano A (1981) Uncompacted myelin lamellae in dysglobulinemic neuropathy. J Neurol Sci 51:131–140
Olsson Y, Sourander P (1969) The reliability of the diagnosis of metachromatic leukodystrophy by peripheral nerve biopsy. Acta Paediatr Scand 58:15–24
Pappenheimer AM, McGill DM (1973) Diphtheria - recent studies have clarified the molecular mechanism involved in its pathogenesis. Science 182:352–358
Pereira JA, Lebrun-Julien F, Suter U (2012) Molecular mechanisms regulating myelination in the peripheral nerve. Trends Neurosci 35:123–134
Peterson AC, Bray GM (1984) Hypomyelination in the peripheral nervous system of shiverer mice and shiverer-normal chimera. J Comp Neurol 227:348–356
Pleasure DE, Towfighi J (1972) Onion bulb neuropathies. Arch Neurol 26:289–301
Pleasure DE, Feldmann B, Prockop DH (1973) Diphtheria toxin inhibits the synthesis of myelin proteolipid and basic proteins by peripheral nerves in vitro. J Neurochem 20:81–90
Pollard JD, King RHM, Thomas PK (1975) Recurrent experimental allergic neuritis. J Neurol Sci 24:365–383
Pollard JD, MacLeod JG, Gatenby P et al (1983) Prediction of response to plasma exchange in chronic relapsing polyneuropathy. J Neurol Sci 58:269–287
Pollard JD, McLeod JG, Feeney D (1985) Peripheral neuropathy in IgM kappa paraproteinaemia: clinical and ultrastructural studies in two patients. Clin Exp Neurol 21:41–54
Pollock M, Nukada H, Frith RW et al (1983) Peripheral neuropathy in Tangier disease. Brain 106:911–928
Prineas JW (1972) Acute idiopathic polyneuritis. An electron microscope study. Lab Invest 26:133–147
Prineas JW (1981) Pathology of the Guillain-Barre syndrome. Ann Neurol 9(suppl):6–19
Quintes S, Goebbels S, Saher G et al (2010) Neuron-glia signaling and the protection of axon function by Schwann cells. J Peripher Nerv Syst 15:10–16
Raine CS (1977) Schwann cell responses during recurrent demyelination and their relevance to onion bulb formation. Neuropathol Appl Neurobiol 3:453–470
Raine CS, Bornstein MB (1979) Experimental allergic neuritis. Ultrastructure of serum induced myelin aberration in peripheral nervous system cultures. Lab Invest 40:423–432
Reich F (1903) Uber eine neue granulation in den nervenzellen. Arch Anat Physiol (Physiol Abt) 27:208–214
Robson JT (1951) Protagon granules in the normal sciatic nerve with some observations on the greater splanchnic nerve. J Neuropathol Exp Neurol 10:77–81
Ropte S, Scheidt P, Friede RL (1990) The intermediate dense line of the myelin sheath is preferentially accessible to cations and is stabilized by cations. J Neurocytol 19:242–252
Rosen JL, Brown MJ, Hickey WF et al (1990) Early myelin lesions in experimental allergic neuritis. Muscle Nerve 13:629–636
Rostami AM (1993) Pathogenesis of immune-mediated neuropathies. Pediatr Res 33(suppl 1):S90–S94
Said G, Hontebeyrie-Joskowicz M (1992) Nerve lesions induced by macrophage activation. Res Immunol 143:589–599
Said G, Boudier L, Zingraff J et al (1983) Different patterns of uremic polyneuropathy: a clinicopathologic study. Neurology 33:567–574, Figure 8

Said G, Ropert A, Faux N (1984) Length dependent degeneration of fibrils in Portuguese amyloid neuropathy. Neurology 34:1025–1032
Saida T, Saida K, Lisak RP et al (1982) In vivo demyelinating activity of sera from patients with Guillain-Barre syndrome. Ann Neurol 11:69–75
Salzer JL, Brophy PJ, Peles E (2008) Molecular domains of myelinated axons in the peripheral nervous system. Glia 56:1532–1540
Schlaepfer WW (1974) Axonal degeneration in the sural nerves of cancer patients. Cancer 34:371–381
Schlaepfer WW, Myers FK (1973) Relationship of internode elongation and growth in the rat sural nerve. J Comp Neurol 147:255–266
Scherer SS, Wrabetz L (2008) Molecular mechanisms of inherited demyelinating neuropathies. Glia 56:1578–1589
Scherer SS (1999) Nodes, paranodes, and incisures: from form to function. Ann N Y Acad Sci 883:131–142
Schroder JM, Himmelmann F (1992) Fine structural evaluation of altered Schmidt-Lanterman incisures in human sural nerve biopsies. Acta Neuropathol 83:120–133
Schroder JM, Sommer C (1991) Mitochondrial abnormalities in human sural nerves: fine structural evaluation of cases with mitochondrial myopathy, hereditary and non-hereditary neuropathies, and review of the literature. Acta Neuropathol 82:471–482
Sharma AK, Thomas PK (1975) Quantitative studies on age changes in unmyelinated nerve fibers in the vagus nerve in man. In: Kunze K, Desmedt JE (eds) Studies on neuromuscular diseases. S Karger, Basel, pp 211–219
Shetty VP, Antia NH, Jacobs JM (1988) The pathology of early leprous neuropathy. J Neurol Sci 88:115–131
Smith KJ, Hall SM (1988) Peripheral demyelination and remyelination initiated by the calcium-selective ionophore ionomycin: in vivo observations. J Neurol Sci 83:37–53
Stoll G, Schwendemann G, Heininger K et al (1986) Relation of clinical, serological, morphological, and electrophysiological findings in galactocerebroside-induced experimental allergic neuritis. J Neurol Neurosurg Psychiatry 49:258–264
Stoll G, Schmidt B, Toyka KV et al (1991) Expression of the terminal complement complex (C5b-9) in autoimmune-mediated demyelination. Ann Neurol 30:147–155
Sumi SM, Farrell DF, Knauss TA (1983) Lymphoma and leukemia manifested by steroid-responsive polyneuropathy. Arch Neurol 40:577–582
Suter U, Welcher AA, Ozcelik T et al (1992) Trembler mouse carries a point mutation in a myelin gene. Nature 356:241–244
Suter U, Welcher AA, Snipes GJ (1993) Progress in the molecular understanding of hereditary peripheral neuropathies reveals new insights into the biology of the peripheral nervous system. Trends Neurosci 16:50–56
Suzuki K, DePaul LD (1972) Myelin degeneration in sciatic nerve of rats treated with hypocholesterolemic drug AY9944. Lab Invest 26:534–539
Svaren J, Meijer D (2008) The molecular machinery of myelin gene transcription in Schwann cells. Glia 56:1541–1551
Taveggia C, Zanazzi G, Petrylak A et al (2005) Neuregulin-1 type III determines the ensheathment fate of axons. Neuron 47:681–694
Thomas PK (1993) Phytanic acid storage disease: pathology of Refsum's disease. In: Dyck PJ, Thomas PK et al (eds) Peripheral neuropathy, 3rd edn. WB Saunders, Philadelphia, pp 28–73
Thomas PK, King RHM (1974) Peripheral nerve changes in amyloid neuropathy. Brain 97:395–406
Thomas PK, Young JZ (1949) Internode length in the nerves of fishes. J Anat 83:336–350
Thomas PK, King RHM, Sharma AK (1980) Changes with age in the peripheral nerves of the rat. An ultrastructural study. Acta Neuropathol 52:1–6
Thomas PK, Berthold CH, Ochoa J (1993) Microscopic anatomy of the peripheral nervous system. In: Dyck PJ, Thomas PK et al (eds) Peripheral neuropathy, 3rd edn. WB Saunders, Philadelphia, pp 28–73
Trapp BD (1990) Myelin-associated glycoprotein. Location and potential functions. Ann N Y Acad Sci 605:29–43
Trapp BD, McIntyre JJ, Quarles RH et al (1979) Immunocytochemical localization of rat peripheral nervous system myelin proteins: P2 protein is not a component of all peripheral nervous system myelin sheaths. Proc Natl Acad Sci U S A 76:3552–3556
Vallat JM, Vital C, Vallat M et al (1973) Neuropathie peripherique a la vincristine. Etude ultrastructurale d'une biopsies due muscle et du nerf peripherique. Rev Neurol 129:365–368
Vallat JM, Leboutet MJ, Jauberteau MO et al (1994) Widenings of the myelin lamellae in a typical Guillain-Barre syndrome. Muscle Nerve 17:378–380
Vital C, Vallat JM (1987) Ultrastructural study of the human diseased peripheral nerve, 2nd edn. Elsevier, New York
Vital C, Staeffen J, Series C et al (1978) Relapsing polyradiculitis after portocaval anastomosis. Eur Neurol 17:108–116
Vital C, Bonnaud E, Arne L et al (1975) Polyradiculonevrite au cours d'une leucemie lymphoide chronique. Etude ultrastructurale d'une biopsie de nerf peripherique. Acta Neuropathol 32:169–172
Vital C, Brechenmacher C, Reiffers J et al (1983) Uncompacted myelin lamellae in two cases of peripheral neuropathy. Acta Neuropathol 60:252–256
Vital C, Brechenmacher C, Cardinaud JP et al (1985) Acute inflammatory demyelinating polyneuropathy in a diabetic patient: predominance of vesicular disruption in myelin sheaths. Acta Neuropathol 67:337–340
Vital C, Dumas P, Latinville D et al (1986) Relapsing inflammatory demyelinating polyneuropathy in a diabetic patient. Acta Neuropathol 71:94–99
Vital A, Vital C, Brechenmacher C et al (1990) Chronic inflammatory demyelinating polyneuropathy in childhood: ultrastructural features of peripheral nerve biopsy in four cases. Eur J Pediatr 149:654–658
Vital A, Latinville D, Aupy M et al (1991) Inflammatory demyelinating lesions in two patients with IgM monoclonal gammopathy and polyneuropathy. Neuropathol Appl Neurobiol 17:415–420
Vital A, Vital C, Julien J et al (1992) Occurrence of active demyelinating lesions in children with hereditary motor and sensory neuropathy (HMSN) type I. Acta Neuropathol 84:433–436, figure 2
Vital C, Gherardi R, Vital A et al (1994) Uncompacted myelin lamellae in polyneuropathy, organomegaly, endocrinopathy, M-protein and skin changes syndrome. Ultrastructural study of peripheral nerve biopsy from 22 patients. Acta Neuropathol 87:302–307
Waxman SG (1980) Determinants of conduction velocity in myelinated nerve fibers. Muscle Nerve 3:141–150
Wayne Moore GR, Raine CS (1988) Immunogold localization and analysis of IgG during immune-mediated demyelination. Lab Invest 59:641–648
Webster D d F (1993) Development of peripheral nerve fibers. In: Dyck PJ, Thomas PK et al (eds) Peripheral neuropathy, 3rd edn. WB Saunders, Philadelphia, pp 243–266
Webster H d F, Spiro D (1960) Phase and electron microscopic studies of experimental demyelination I. Variations in myelin sheath contour in normal guinea pig sciatic nerve. J Neuropathol Exp Neurol 19:42–69
Weinberg H, Spencer PS (1976) Studies on the control of myelinogenesis II. Evidence for neuronal regulation of myelinogenesis. Brain Res 113:363–378
Weller RO, Herzog I (1970) Schwann cell lysosomes in hypertrophic neuropathy and in normal human nerves. Brain 93:347–356
Wiley CA, Ellisman MH (1980) Rows of dimeric particles within the axolemma and juxtaposed particles within glia, incorporated into a new model for the paranodal glial-axonal junction at the Node of Ranvier. J Cell Biol 84:261–280
Wiley-Livingston CA, Ellisman MH (1980) Development of axonal membrane specializations defines nodes of Ranvier and precedes Schwann cell myelin elaboration. Dev Biol 79:334–355

Williams PL, Hall SM (1971) Prolonged in vivo observations of normal peripheral nerve fibres and their acute reactions to crush and deliberate trauma. J Anat 108:397–408

Windebank AJ, Dyck PJ (1984) Lead intoxication as a model of primary segmental demyelination. In: Dyck PJ, Thomas PK et al (eds) Peripheral neuropathy, 2nd edn. W.B. Saunders, Philadelphia, pp 650–665

Wisniewski H, Prineas J, Raine CS (1969) An ultrastructural study of experimental demyelination and remyelination, part I. Lab Invest 21:105–118

Woodhoo A, Sommer L (2008) Development of the Schwann cell lineage: from the neural crest to the myelinated nerve. Glia 56:1481–1490

Yiannikas C, McLeod JG, Pollard JD, Baverstock J (1986) Peripheral neuropathy associated with mitochondrial myopathy. Ann Neurol 20:249–257

Yoshikawa H, Dyck PJ (1991) Uncompacted inner myelin lamellae in inherited tendency to pressure palsy. J Neuropathol Exp Neurol 50:649–657